Antimicrobial activities of phenoloxidase-generated reactive compounds and regulation of immune response by a serpin from *Manduca sexta*

By

PICHENG ZHAO

Bachelor of Engineering in Biochemical Engineering
East China University of Science and Technology
Shanghai, China
2001

Submitted to the Faculty of the
Graduate College of the
Oklahoma State University
in partial fulfillment of
the requirements for
the Degree of
DOCTOR OF PHILOSOPHY
December, 2010

Antimicrobial activities of phenoloxidase-generated reactive compounds and regulation of immune response by a serpin from *Manduca sexta*

Dissertation Approved:

Dr. Haobo Jiang

Dissertation Adviser

Dr. Jack Dillwith

Dr. Stephen Marek

Dr. Andrew Mort

Dr. Gordon Emslie

Dean of the Graduate College

ACKNOWLEDGMENTS

I want to first express my gratitude to Dr. Haobo Jiang. As my advisor, he helped me with courses, research projects and career development and also provided support for my personal life development. He gave me many advices and showed a lot of patience, and I profited a lot from study and work in his laboratory.

I would also like to thank my committee members: Drs. Jack Dillwith, Stephen Marek, and Andrew Mort, who provided useful suggestions on courses and some research supports, such as chemical reagents, microbial strains, and equipment usages.

I appreciate the faculty, staff, and student body in the Department of Entomology and Plant Pathology at OSU. I learned a lot from the courses. With their helps, my study went well. I want to thank my classmates and other students in the department for sharing their knowledge, experience, and friendship with me.

I want to say thanks to Yang Wang, our lab technician. She offered me all kinds of technical supports. I also learned many things from my labmates, Zhen Zou, Zhiqiang Lu, Subrahanmanyam Rayaprolu, Siwei Liu, Sumathipala Niranji, Fan Yang, Yinxia Hu, Shuguang Zhang and Xiufeng Zhang, and enjoyed working with them. I appreciate the services of OSU Recombinant DNA/Protein Core Facility. I obtained DNA sequence data from Lisa Whitworth and protein mass fingerprint results from Dr. Steve Hartson and Janet Rogers. I also got bioinformatics support from Hua Wen and Yan Song. In the cell-

related work, I was helped by Pingsheng Luoguan, Yujie Guo, Lin Liu, Amy Cragun, and Jerry Ritchey. I would not have achieved my research goals without these assistances.

Finally I would like to express my appreciations to my wife Jiajing Li, who took good care of me and shared my happiness and stress, to my parents Shiwang Zhao and Saibao Li, who supported me all the time, and to my son Roy Zhao, who brought so much fun to my life.

TABLE OF CONTENTS

Chapter Page

Chapter Page

LIST OF TABLES

LIST OF FIGURES

Figure Page

Figure Page

Figure Page

Figure Page

CHAPTER I

INTRODUCTION

Insects survive from wounding and microbial infection in a natural environment. Lacking acquired immunity mammals have, they rely solely on innate immunity to fend off pathogens. Although being regarded as primitive, innate immunity forms the foundation of acquired immunity, exists in all animals, and shares certain features with plant defense responses. Innate immunity works as the first line of defense against pathogens in mammals and it acts as the entire defense system to fight off infection in insects. This system is artificially divided into two components: cellular and humoral. Cellular responses are phagocytosis, nodulation and encapsulation, whereas humoral responses in general include pathogen recognition, prophenoloxidase (PPO) activation, cytokine generation, and the antimicrobial peptide (AMP) effect. Effector proteins of the humoral responses come from regulated gene expression in cells, and some of them aid in initiating nodulation and encapsulation. In other words, cellular immunity and humoral immunity are closely associated with each other.

An insect immune reaction generally involves fat body, hemocytes, and plasma factors [Gillespie et al., 1997; Lavine et al., 2002; Kanost et al. 2004]. Fat body and hemocytes are major sources of immunity-related molecules in the circulation and on the surface of immune cells. These include killing molecules (*e.g.* AMPs), microbial

recognizers (*e.g.* recognition proteins of pathogen-associated molecular patterns), signaling transducer (*e.g.* Toll like receptors), and immune reaction modulators (*e.g.* serine protease inhibitors). AMPs bind to microbes and cause leakage and death of the cells. Pattern recognition proteins associate with pathogen-associated molecular patterns (PAMPs) to sense the invading microbes and relay the immune challenge signal to the defense system. The extracellular signal mediators and modulators lead to proper responses by producing, for instance, active enzymes that generate chemicals for wound healing and microbe killing. We can apply genetic and biochemical methods to analyze these processes individually in order to understand their intricate relationships.

The PPO activation cascade is a part of the humoral immunity response. Active insect POs, also known as tyrosinase-type POs, are believed to have the oxygenase-oxidase active site and play a role in microbe killing, cuticle sclerotization, wound healing, catalyze the production of quinones and melanin formation [Ashida and Brey, 1997]. Due to the chemical reactivity and presumed cytotoxicity of these compounds, this proteolytic cascade is likely related to immobilization and elimination of invading pathogens [Sugumaran, 2002; Cerenius and Söderhäll, 2004; Nappi and Christensen, 2005]. However, there is no direct evidence that reactive compounds generated by PO contribute to microbe killing: active PO has never been purified for *in vitro* analysis [Söderhäll and Cerenius, 1998]. Leclerc et al. [2006] reported that a *Drosophila* strain with a defect in the PPO activation protease-1 (PAE1) is somewhat resistant to microbial infection. It seems questionable if active PO really takes part in extermination of microbes. *In vivo* and *in vitro* studies demonstrate that POs generate quinones for melanization [Jiang et al., 2003; De Gregorio et al., 2002] and change the physical

properties of hemolymph clots, perhaps via protein cross-linking [Bidla et al., 2005]. Cuticle tanning, as demonstrated in the beetle *Tribolium castaneum*, involves laccase-2 rather than tyrosinase-type POs [Arkane et al., 2005]. With the understanding of PPO activation cascade, we generated *M. sexta* PO *in vitro* and tested its antimicrobial activity by using dopamine as substrate. At the same time, we confirmed this activity came from one of the intermediates from PO catalyzed dopamine oxidization process. We also discussed the mode of action of this toxic product. All these results can be regarded as evidence to confirm the important role of PO in insect immunity.

Extracellular and intracellular immune pathways are regulated at different levels including gene transcription, mRNA stability, translation, and post-translational modifications. The regulation of enzyme activity by proteolytic cleavage of its zymogen is a post-translational modification mediated by specific serine proteases. The PPO activation cascade is composed of multiple serine proteases, some of which are controlled by a superfamily of serine protease inhibitors named serpins. Many serpins form inactive covalent complex with their target proteases. A key part of serpin is its reactive site loop specifically recognized by its target enzyme. The enzyme-inhibitor binding leads to the loop cleavage between P1 and P1' sites [Schecter and Berger, 1967]. The acyl-enzyme complex undergoes a conformational change where the unstressed loop inserts into β-sheet A as strand 4A. The dragging of the protease to the other side of the inhibitor and distortion of its catalytic machinery cause the covalently linked enzyme to irreversibly lose its activity. We have identified a new serpin, *M. sexta* serpin-10, in an EST sequencing project [Zou et al., 2008]. BLAST search indicates serpin-10 may have a close evolutionary relationship with plasminogen activator inhibitors (PAIs) in mammals.

There are many serpin genes in one insect genome. For example, in the genome of another lepidopteran insect, *Bombyx mori*, there are 34 serpin genes (Fig. 1) [Zou et al., 2009]. Different serpins inhibit the activity of their corresponding target serine proteases,

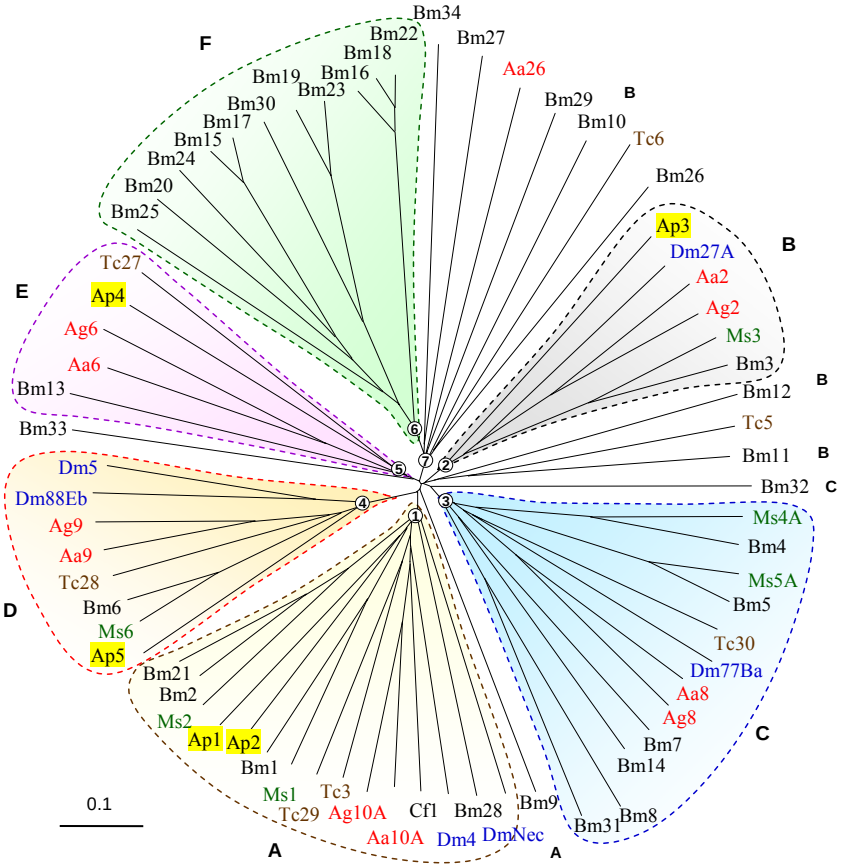

Figure 1. Phylogenetic relationships among the serpins from *B. mori*, *M. sexta*, *D. melanogaster*, and other insects. Bootstrap values for nodes 1 through 7 are 854, 973, 784, 1000, 660, 993, and 771, respectively (1000 trials). The corresponding clades form six distinct phylogenetic groups named A through F [Zou et al., 2009].

which may be involved in the immune response. By studying *M. sexta* serpin 10, we tried to look for its target protease, which may finally lead to some interesting findings.

This work is composed of two parts. We are trying to study the antimicrobial ability of PO, substrate and generated reactive compounds and to reveal a possible

relationship between serpin10 with *M. sexta* immune responses.

CHAPTER II

REVIEW OF LITERATURE

2.1 An overview of insect innate immunity

The process of insect immune responses can be divided into four parts: initiation, amplification, execution and regulation. The initiation requires proteins that recognize and report invading microorganisms. The alarm passes through extracellular proteins and into immune cells. Through these signaling pathways, immunity-related genes are transcribed and translated into proteins. The effectors include antimicrobial peptides and POs which participate in the killing of microorganisms. The pathways are modulated.

2.2 Pattern recognition proteins in insects

Pattern recognition proteins are guards of the defense system. They recognize pathogen components known as pathogen-associated molecular patterns (PAMPs) with certain levels of specificity. Pattern recognition proteins exist in plasma, on cell membranes, or in the cytosol sometimes. Some are classical membrane receptors, some have enzyme activities, and some even directly kill microbes. According to the PAMPs they recognize and sequence homology, pattern recognition proteins are divided into different families [Akira et al., 2001; Lata and Raghava, 2008].

A founding member of the peptidoglycan recognition proteins (PGRPs) was discovered in plasma of the silkworm through traditional protein purification and functio-

nal assay. These proteins, now including cell surface receptors, recognize bacterial peptidoglycans. Especially in Gram-positive bacteria, Lys-type peptidoglycans are abundant, composing almost 50% of the cell wall. In Gram-negative bacteria, DAP-type (meso-diaminopimelic acid (DAP) as the third amino acid) peptidoglycans form a relatively thin layer beneath the lipopolysaccharide (LPS). In *D. melanogaster*, DAP-type peptidoglycans are recognized by PGRP-LC while Lys-type peptidoglycans by PGRP-SA. The interaction of PGRPs and peptidoglycans triggers several immune pathways. The amidase or carboxypeptidase activity of some PGRPs breaks down peptidoglycans and cause bacterial death. Some mammalian PGRPs are reported to have bactericidal activity without the peptidoglycan-hydrolytic activity [Royet et al., 2007]. In some insects, peptidoglycan-bound PGRPs trigger the proPO pathway [Kim et al., 2008]. While PGRPs are homologous to T7 lysozyme, breakdown of highly cross-linked peptidoglycans is assisted by other peptidoglycan-hydrolyzing enzymes homologous to chicken lysozyme. Without the latter, PGRPs may not get access to peptidoglycan and carry on further hydrolysis or signaling amplification. *D. melanogaster* PGRP-LC and -SC1 are believed to be related to phagocytosis by working as adaptors [Royet et al., 2007].

In *Drosophila* and other insects, another group of pattern-recognition proteins named GNBPs recognize Gram-negative bacterial cell wall component LPS and fungal cell wall component β-1,3-glucan [Kim et al., 2000]. Sequence comparison reveals that GNBPs and β-1,3-glucan-binding proteins form a protein family related to bacterial and insect glucanases. GNBPs are believed to stimulate further immune responses although no downstream signal acceptor has been reported yet. From unpublished data in our lab,

GNBP specifically binds DAP-peptidoglycans and triggers the activation of proHP14 in *M. sexta*. The activated HP14 can initiate the proPO system, finally leading to melanization and microbe killing [Kim et al., 2000; Wang and Jiang, 2006].

2.3 Prophenoloxidase (PPO) activation cascade in *M. sexta* and *Tenebrio molitor*

The PPO cascade is a part of the extracellular serine protease network which also processes spätzle for Toll pathway activation (Fig. 2). These proteases are produced as inactive zymogens to be sequentially activated by recognition of PAMPs. Gram-positive

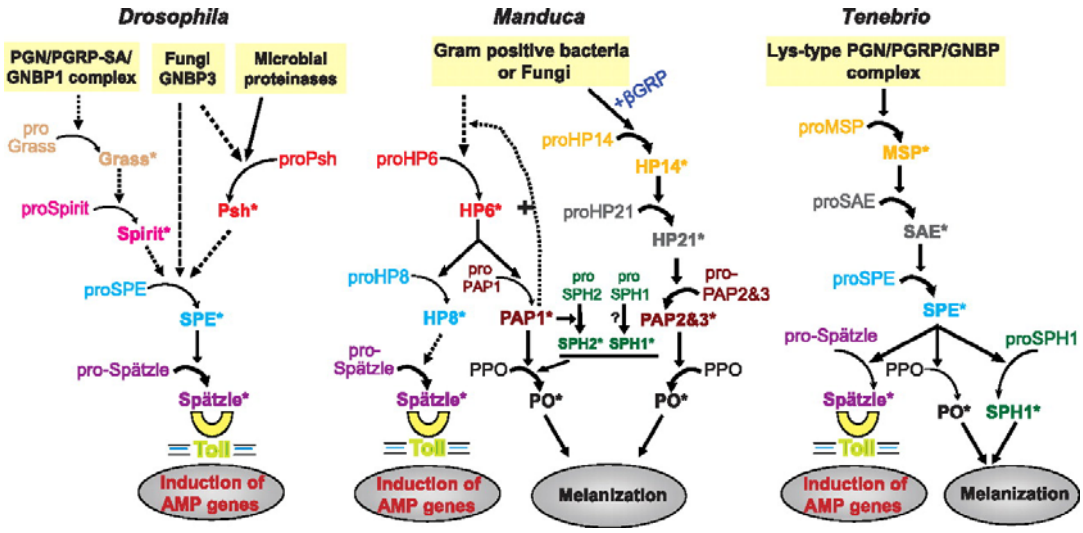

Figure 2. A model for the roles of *M. sexta* HP6 and HP8 in extracellular immune pathways and comparison with *Drosophila* and *Tenebrio* innate immune pathways involving serine protease cascades. Arrows indicate activation of downstream components or steps. Dashed arrows indicate steps that have not been experimentally verified or in which components of the pathway have not yet been identified. Proteins shown in the same color are putative orthologs. PGN, peptidoglycan; PGRP, peptidoglycan recognition protein; PGRP-SA, peptidoglycan recognition protein-SA; βGRP, β-1,3-glucan recognition protein; GNBP, Gram-negative bacteria binding protein; PPO, prophenoloxidase; SAE, SPE activating enzyme; Psh, Persephone. [An et al., 2009]

bacteria and fungi, bound with PGRP-SA and βGRP, cause autoactivation of proHP14. Then HP14 activates HP21, which somehow leads to activation of HP1, HP6 and HP17 (Fig. 3). HP6 activates HP8 and PAP1 [An et al., 2009], whereas HP21 directly activates

PAP2 and PAP3 [Wang and Jiang, 2007; Gorman et al., 2007]. One or more of these PAPs, assisted by serine protease homologs (SPHs), cleaves proPO to form active PO. PO catalyzes the formation of quinones, precursors of melanin [An et al., 2009]. The activation of these zymogens is all caused by proteolytic cleavage at a specific site, which induces a conformational change that exposes the substrate binding site for catalysis [Kanost et al., 2004]. The protease network is strictly regulated by serine protease inhibitors of the serpin superfamily (Fig. 3) [Tong et al., 2005; Tong and Kanost, 2005].

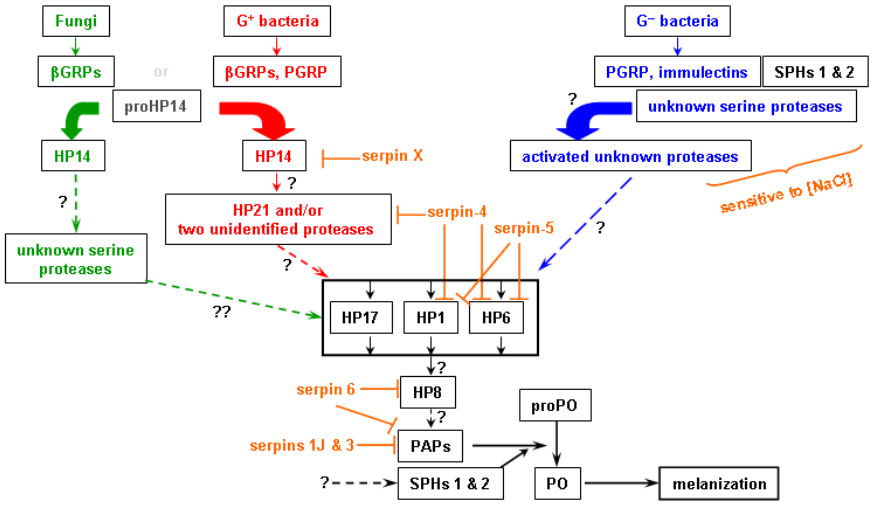

Figure 3. PPO activation pathway and its regulation by serpins. *Arrows* indicate activation of downstream components or steps. *Curved arrows* represent autoactivation of initiating proteases. *Dashed arrows* indicate potentially more than one step. *Arrows* labeled with "?" indicate steps that have not been experimentally verified. Regulation of proteases by serpins is indicated. Two unidentified serpins that regulate HP14 and HP8 are labeled as *X* and *Y*, respectively. [Tong et al., 2005]

The research on *T. molitor* shows that the beetle employs a slightly different proteolytic enzyme cascade to activate PPO (Fig. 2). In the presence of Ca^{2+}, the PAMP Lys-type PG forms a complex with Tm-PGRP-SA and Tm-GNBP1. This complex is required for the activation of Tm-MSP zymogen, the ortholog of HP14. Activated Tm-

MSP cleaves Tm-SAE, the ortholog of *M. sexta* HP21, whereas Tm-SAE activates Tm-SPE, the ortholog of *M. sexta* HP8. The active SPE then cleaves and activates SPH1, PO and Spätzle precursors to trigger both melanization and Toll pathway [Kim et al., 2008; Kan et al., 2008]. It is interesting that the activation of PPO here doesn't require specific PPO activating enzyme. Tm-SPE (Spätzle-processing enzyme), as a universal activator working on different zymogen substrates, activates PPO directly.

Insect POs, or tyrosinase-type phenoloxidases, are similar to mammalian tyrosinases in having two catalytic activities: the oxygenase activity hydroxylates monophenols to *o*-diphenols and the oxidase activity converts *o*-diphenols to quinones (Sugumaran, 2002; Nappi and Christensen, 2005). While tyrosine formed dopachrome in the presence of *M. sexta* PO (Aso et al., 1985), it is unclear if the hydroxylation step is catalyzed by PO itself or other enzymes in the preparation, such as tyrosine hydroxylase or peroxidase. Despite the uncertainty, due to its well established *o*-diphenoloxidase activity, PO was proposed to take part in melanin formation, wound healing, cuticle sclerotization, and microbe killing (Ashida and Brey, 1998). *In vitro* and *in vivo* studies demonstrated that PO generates quinones for melanogenesis (Jiang et al., 1998; De Gregorio et al., 2002) and leads to changes in the physical properties of hemolymph clot through protein crosslinking (Birla et al., 2005). Cuticle tanning (*i.e*. pigmentation and sclerotization) was attributed to *Tribolium castaneum* laccase-2 rather than a tyrosinase-type PO in the beetle (Arakane et al., 2005). Therefore, we decided to test the most controversial function of PO by directly measuring possible antimicrobial activity of the reactive compounds produced *in vitro* by this enzyme. We first used purified *M. sexta* proPO-activating proteinase-3 (PAP-3) and serine proteinase homolog-1 and -2 (SPH-1

and -2) to activate proPO – the SPHs are needed to accompany PAP and proPO in the cleavage activation (Gupta et al., 2005). Quinones were generated by active PO from its natural substrate, dopamine. After treating microbes with the reaction mixture, we determined morphology, survival, and growth of the cells and established that the reactive intermediates yielded by PO had a broad-spectrum bactericidal activity. In addition to that, we studied the enzymatic activities of *M. sexta* PO and the nature of its antimicrobial products.

2.4 Signaling pathways of insect immunity

Transferring signal from extracellular into intracellular, Toll, Imd and JNK signaling pathways widely exist in vertebrates and invertebrates. In insects they are best understood in *Drosophila* [Lemaitre and Hoffmann, 2007]. Comparative genomic research indicates components of these pathways are well conserved in other insects, such as *Anopheles gambiae, Apis mellifera, Aedes aegypti, Tribolium castaneum,* and *Bombyx mori* [Christophides et al., 2002; Zou et al., 2007; Tanaka et al., 2008; Cheng et al., 2008]. These pathways are mainly composed of PAMP recognition proteins, proteases, cell surface receptors, intracellular kinases, and transcription factors. Through cross-talks, different pathways may co-regulate a common set of target genes [Aggarwal and Silverman, 2008].

2.4.1 Toll pathway *in Drosophila*

The *Drosophila* Toll pathway is similar to the mammalian one, but they differ in some ways. The most distinct feature is that *Drosophila* Toll receptor located on the plasma membrane does not directly recognize PAMPs. Fungal β-1,3-glucan and bacterial Lys-peptidoglycan are recognized by βGRP and PGRP-SA, respectively (Fig. 2).

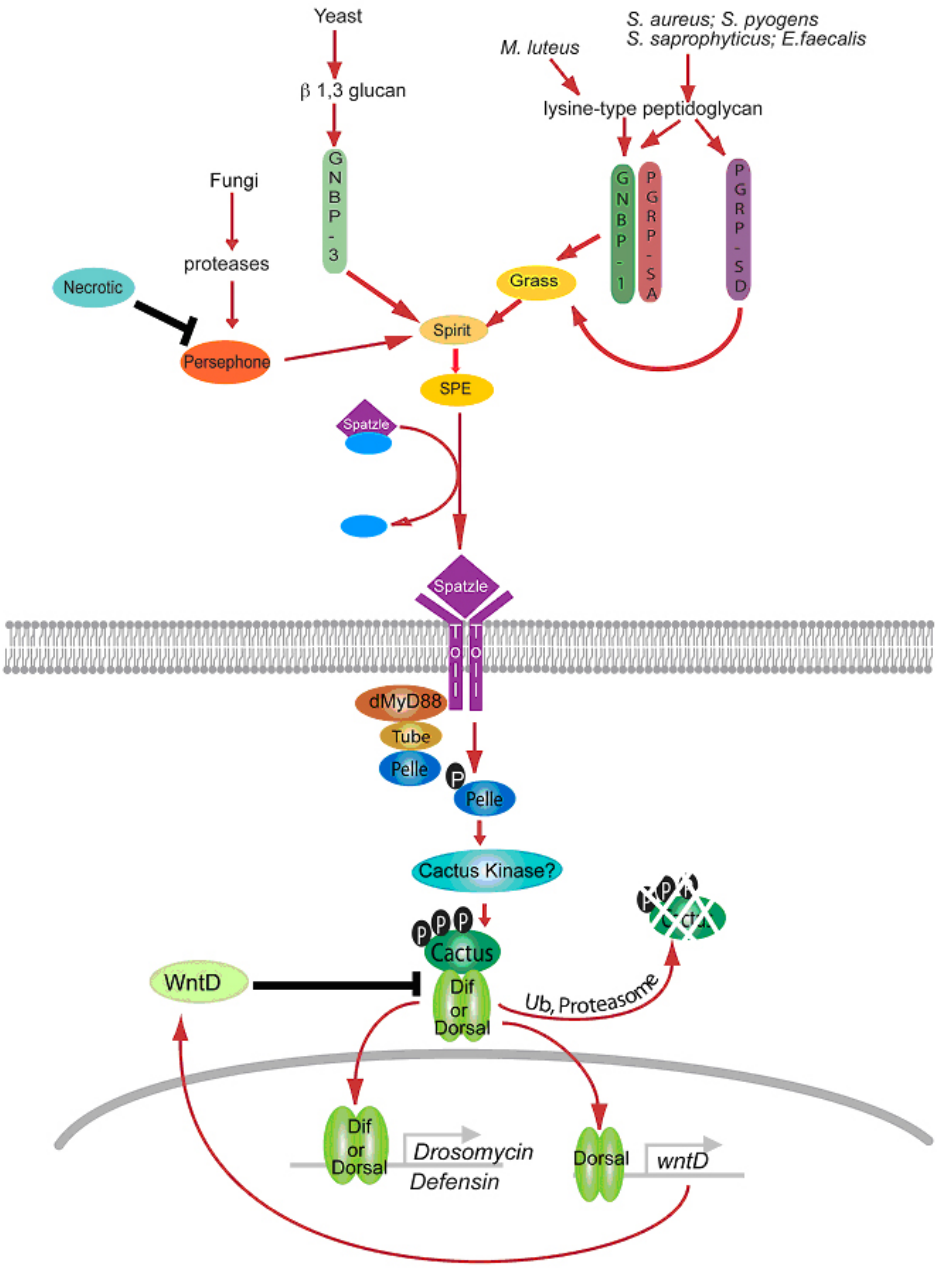

Figure 4: Activation and regulation of the *Drosophila* Toll pathway. Red arrows indicate the Toll signaling cascade, including the three microbial recognition systems and the intracellular signaling cascade, while the black arrows highlight the negative regulators and their likely targets. [Aggarwal and Silverman, 2008]

The binding leads to activation of two chymotrypsin-like serine proteases, Spirit and SPE. Spirit cleaves and activates SPE (Spätzle-processing enzyme) and SPE cleaves Spätzle to form an active ligand of Toll. The interaction of Spätzle and its receptor

transmits the extracellular signal into the cell nucleus via an intracellular pathway (Fig. 4) highly similar to the mammalian one. Toll does not have an enzymatic activity, and it needs adaptor proteins to associate with a kinase. *Drosophila* MyD88 works more like a scaffold protein, which associates with another adaptor protein, Tube, and is recruited by Toll. Tube then recruits Pelle, a kinase homologous to mammalian interleukin-1 receptor-associated kinases. Pelle mediates the phosphorylation and ubiquitinylation of Cactus through phosphorylation of Cactus kinase. The modified Catus disassociates from a preexisting complex with an NF-κB transcriptional factor Dif or Dorsal and is degraded in the proteasome. Freed Dif or Dorsal enters the nucleus to initiate the transcription of immunity-related genes, such as antimicrobial peptides, mediators and regulators (*e.g.* WntD and serpins) of immune response [Aggarwal and Silverman, 2008].

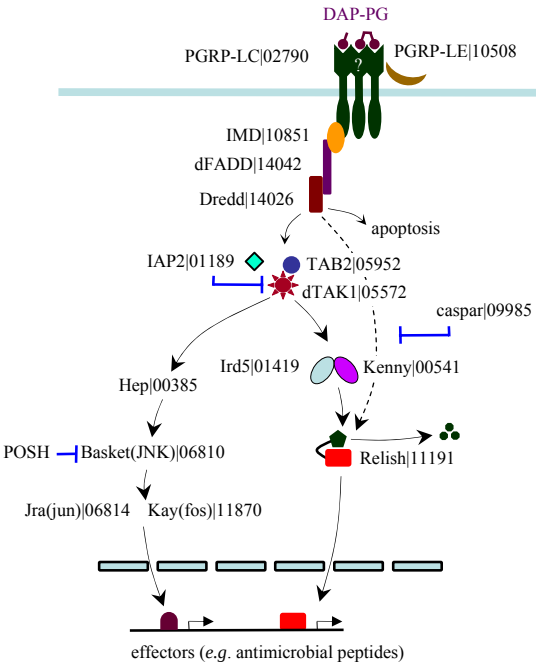

Figure 5. Schematic drawing of the IMD pathway and JNK branch for induced synthesis of immune responsive effectors in *Drosophila* and *Tribolium*. Components of the putative pathways from *T. castaneum* are predicted based on sequence similarity. The *Drosophila* gene names are followed by GLEAN numbers of their beetle orthologs. [Zou et al., 2007]

2.4.2 Imd/JNK pathway in *Drosophila*

Two conjugated branches constitute the Imd/JNK pathway (Fig. 5). The Imd branch is somewhat similar to the Toll pathway. The DAP-type peptidoglycan of Gram-negative bacteria triggers the pathway. The cell surface PGRP-LC recognizes polymeric DAP-PG from outside of the cell, while in the cell PGRP-LE recognizes monomeric fragment of a DAP-type peptidoglycan known as tracheal cytotoxin. PGRP-LC or PGRP-LE may directly interact with IMD and IMD activates TAK1. Then the pathway divides into two branches. In one branch, TAK1 mediates activation of NF-κB transcriptional factor, Relish. Relish initiates the transcription of AMP and other immunity-related genes. In the other branch, JNK is believed to down-regulate the immune gene expression and trigger cell apoptosis through a caspase-8-like protein, DREDD [Aggarwal and Silverman, 2008].

2.5 Regulation of protease-mediated signal transduction by serpins

2.5.1 General introduction and nomenclature of serpins

Among natural protease inhibitors, serpins form the largest superfamily [Rawlings et al., 2004]. They widely exist in eukaryotes and prokaryotes, but their evolutionary relationships are unclear. Some believe ancestral serpins in prokaryotes gave rise to serpins in other prokaryotes and were transferred to eukaryotes. Others believe the prokaryotic serpins are originated in eukaryotes. Serpins from both groups of organisms are functional and critical for survival [Irving et al., 2000; 2002]. Serpins are involved in many human diseases related to serine protease regulation and have been well studied [Potempa et al., 1994; Church et al., 1997]. The research of arthropod serpins and other serine protease inhibitors enhanced our understanding of arthropod immunity, which also

contributed to our understanding of mammalian innate immunity [Kanost, 1999]. Members of the serpin superfamily possess different functions but share a similar structure [Silverman et al., 2000]. Some serpins are able to work as cross-class inhibitors against cysteine proteinases [Barrett et al., 2001; Irving et al., 2002] via the same mechanism of structure transformation [Stein and Chothia, 1991]. The conformation of a serpin is maintained by different structural and functional regions, including three β-sheets (A, B and C), at least seven α-helices, and a flexible reactive center loop (RCL) [Stein and Chothia, 1991; Potempa et al., 1994; Elliot et al., 1996]. There are several important regions for function: a mobility-essential hinge located at about P9-P15 region on RCL [Hopkins et al. 1993], an initiation point breach at the top of β-sheet A, a shutter near β-sheet A center [Whisstock et al., 2000a], and a gate composed of strands 3, and 4 of β-sheet C [Mottonen et al. 1992; Stein and Carrell 1995]. Five different conformational states exist for serpins: native, cleaved, latent, δ, and polymeric [Whisstock et al., 1998]. The deformation of the serpin molecule forces a target protease to go through a conformational change from active to inactive [Huntington et al., 2000].

2.5.2 Inhibitory mechanism of serpins

Serpins are a superfamily of 45-50 kDa proteins, some of which inhibit serine proteases by forming a covalent complex. The target enzymes contain a catalytic center composed of three essential amino acid residues: Ser, His, and Asp (Fig. 6) [Tsukada and Blow, 1985]. Their side chains form a charge relay system to withdraw the hydrogen proton from the hydroxyl group of the catalytic Ser, which attacks the carbonyl carbon of a peptide bond in the inhibitor. The scissile bond (*i.e.,* the bond between P1 and P1' sites) is located on an exposed RCL which fits the substrate binding cleft of its target enzyme.

The nucleophilic attack leads to the formation of a tetrahedral intermediate which becomes an acyl-enzyme complex while the scissile bond breaks. The carboxyl-terminal portion of the inhibitor (product-1) is released from the protease, whereas the amino-terminal portion forms an ester bond with the Ser side chain [Egelund et al., 1998].

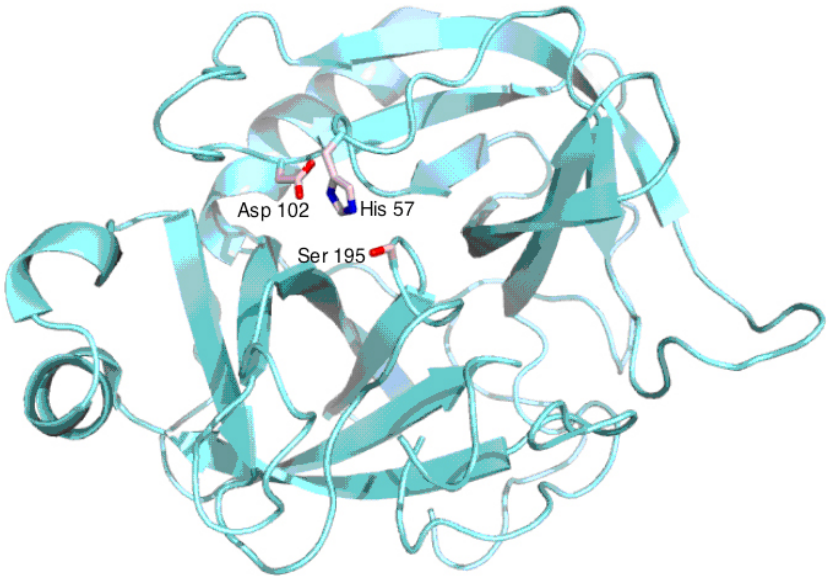

Figure 6. X-ray crystal structure of the archetypal serine protease chymotrypsin (pdb code 4CHA) [Tsukada and Blow, 1985]. The three catalytic residues (His57, Asp102 and Ser195) are labeled.

In the case of substrate, a nitrogen atom on the histidine side chain forms a hydrogen bond with H^+ of an incoming water molecule, and the hydroxyl group of the water substitutes the acyl portion of the substrate on the catalytic serine to release the amino-terminal fragment as product-2. Then the enzyme is ready for another catalytic reaction (Fig. 7). However, when the scissile bond of an inhibitory serpin breaks, there is a stress release of its RCL that incorporates to the major β-sheet A as a new strand (s4A). Because of the ester bond between the serpin P1 residue and protease catalytic Ser, the protease is dragged to the other site of the inhibitor, with its catalytic machinery distorted by the RCL during this spring-like movement. The catalytic His is no longer available for

splitting water and release product-2: the protease is trapped in the acyl-enzyme complex (Fig. 8) [Huntington et al., 2000; Gettins 2002; Whisstock et al., 2000].

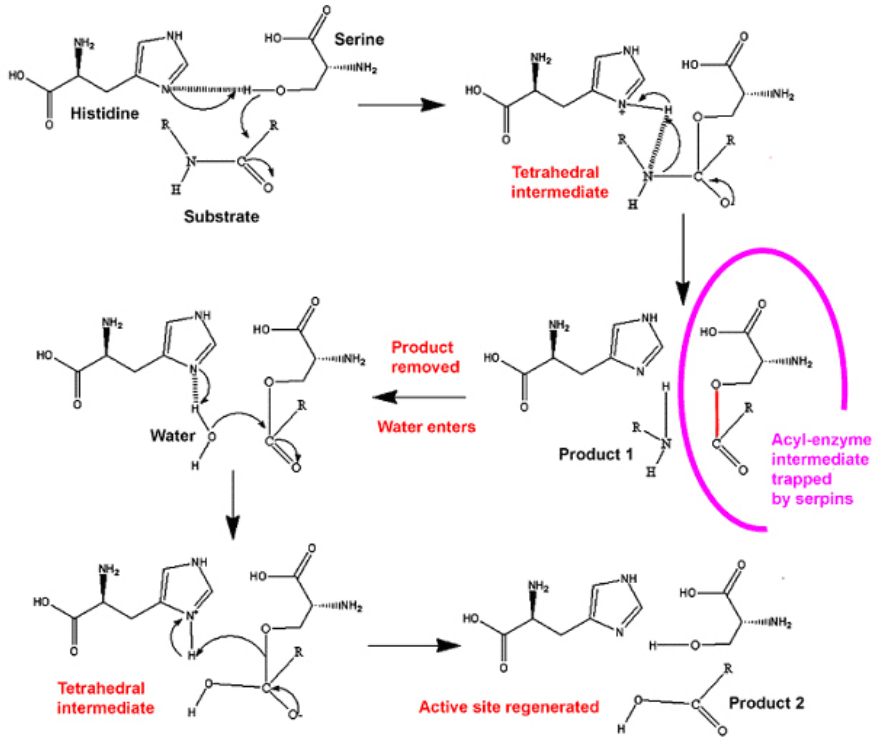

Figure 7. Catalytic mechanism of serine proteases illustrating the stage in the cycle that is trapped by serpin inhibitors (magenta circle).

A serpin at the native state is active and the molecule is metastable or stressed. The RCL is exposed and ready to interact with a target protease. The cleavage at the scissile bond initiates the insertion of a part of the RCL into the β-sheet A and release the stress of molecule [Huntington et al., 2000; Whisstock et al. 2000b]. This stress-to-relax (S-to-R) rearrangement increases the molecule stability [Carrell and Owen, 1985]. In the latent state, a serpin molecule is intact, but its RCL is inserted into β-sheet A. Some serpins (*e.g.*, antithrombin) need a cofactor (*e.g.*, heparin) to maintain its active conformation (Fig. 9) [Whisstock et al. 2000b; Li et al., 2004; Johnson et al., 2004]. When plasminogen activator inhibitor-1 (PAI-1) is expressed in native form but not

bounded with vitronectin, it undergoes a conformational change to latent and become inactive. Formation of latent serpin may be one of the regulatory mechanisms for this family of inhibitors (Fig. 10) [Lindahl et al, 1989; Zhang et al., 2007; Zhang et al., 2008]. The δ and polymeric states, found in mutant serpins, are regarded as misfolded product without inhibitory activity [Gooptu et al., 2000; Berkenpas et al., 1995; Whisstock and Bottomley, 2006].

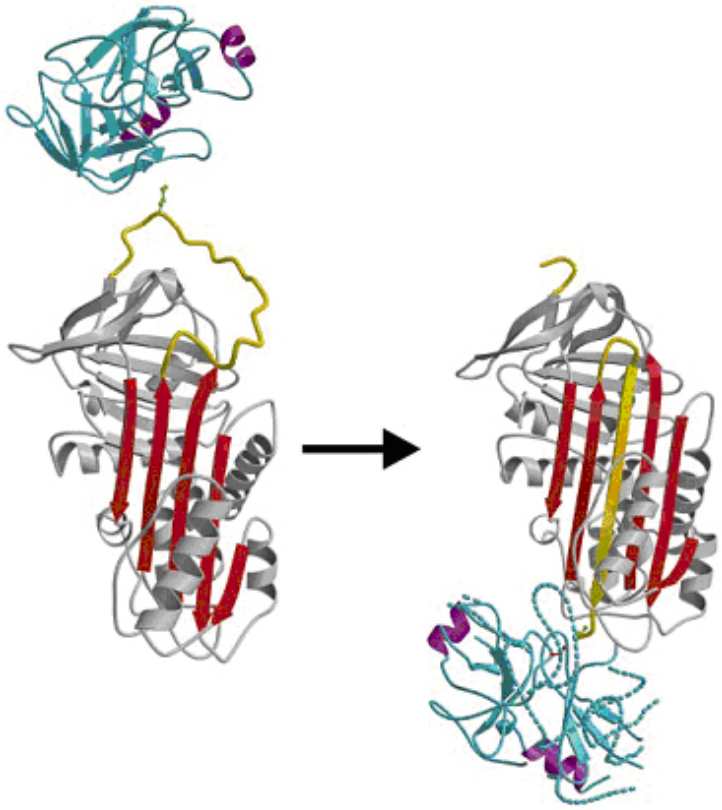

Figure 8. Formation of a serpin-protease complex. Ribbon depictions of native α1-antitrypsin8 with trypsin aligned above it in the docking orientation (left), and of the complex showing the 71Å shift of the P1 methionine of α1-antitrypsin, with full insertion of the cleaved reactive center loop into the A-sheet (right). Regions of disordered structure in the complexed trypsin are shown as interrupted coils projected from the native structure of trypsin. Red, α1-antitrypsin β-sheet A; yellow, reactive-centre loop; green ball-and-stick, P1 Met; cyan, trypsin (with helices in magenta for orientation); red ball-and-stick, active serine 195. [Huntington et al., 2000]

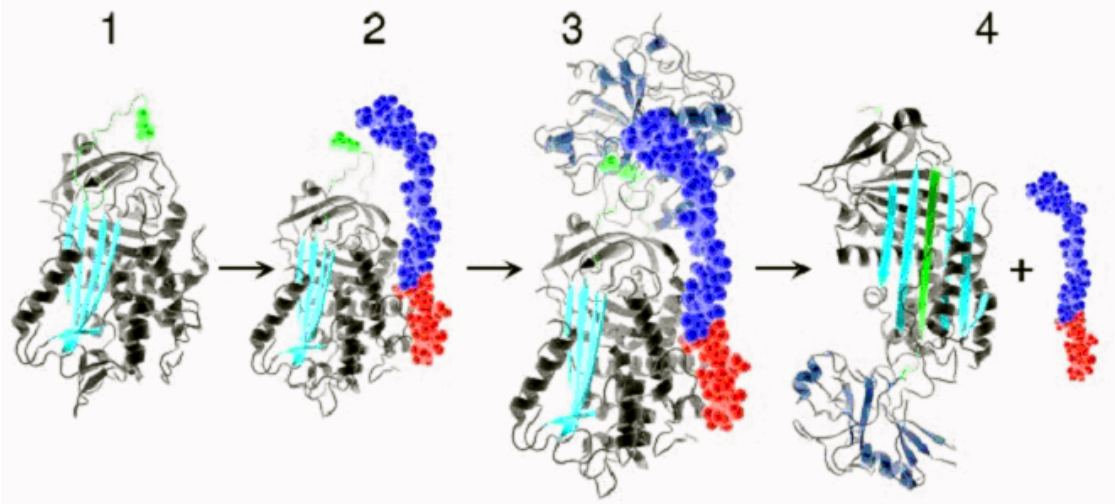

Figure 9. Conformational changes of native antithrombin interacting with heparin and thrombin. From left to right: 1) the partially inserted conformation of native antithrombin. The P1 arginine is in green spheres (from pdb [Skinner et al., 1997]); 2) binding of the high affinity heparin pantasaccharide sequence (in blue spheres) within long chain heparin (in red spheres) (from pdb 1TB6 [Li et al., 2004]). Note how the P1 Arg has flipped to a more exposed position; 3) initial interaction of thrombin (grey) with the RCL. Thrombin also contains a binding site for heparin (from pdb 1TB6); 4) Following docking, the final serpin enzyme complex is formed (illustrated using the antitrypsin/trypsin complex) and heparin is released (Huntinton et al., 2000).

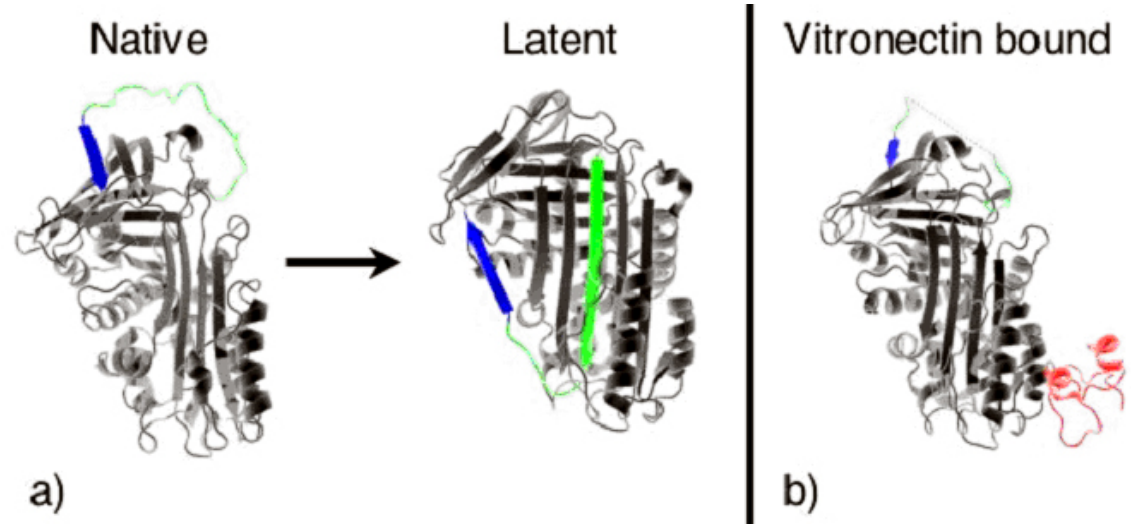

Figure 10. X-ray crystal structure of native, latent, and vitronectin-bound PAI-1. a) X-ray crystal structure of native PAI-1 (from pdb 1DVM [Stout et al, 2000]) (stabilized though mutation). The RCL is in green, and the first β-strand of the C-β-sheet in blue. In the absence of vitronectin, PAI-1 converts to the latent form (right) (from pdb 1LJ5 [Stein et al., 2009]). The first strand of the C-sheet has peeled off to allow full RCL insertion. b) Structure of native PAI-1 bound to vitronectin (in magenta, pdb 1OCO [Yoshikawa et al., 1998]). Part of the RCL is disordered in this structure and is represented by a dashed line.

According to the mechanism of conformational changes, we can divide a serpin molecule into rigid regions, hinge and plastic deformation regions. The rigid regions may have integral shift during conformational remolding but have no structure change. They provide a scaffold or structural core for the molecule. The hinge region requires flexibility for rotation, whereas the deformation region needs to maintain the native active state at first and ready for S-to-R transition. Therefore, conservation of sequence features is essential within these critical regions [Irving et al., 2000; Whisstock et al. 2000a]: the hinge region of inhibitory serpin has a glycine at P15 always, a threonine or serine at P14 usually, and alanine, glycine, or serine (residues with short side chains) at P9–P12 [Hopkins et al. 1993]. A cluster of conserved residues within the breach is essential for a hydrogen bond network [Harrop et al., 1999; Li et al., 1999]. These conserved residues allow the RCL to insert into the β-sheet A rapidly and efficiently. A mutation within the shutter region always causes the serpin dysfunction, while mutation in the hinge region often turns inhibitory serpin into a substrate [Irving et al., 2000; Whisstock et al. 2000a].

2.5.3 Clearance and uptake of serpin-enzyme complexes

As described above, a serpin and its target protease form a covalently-linked complex that is stable in SDS. Besides being cleared up from the circulation, some serpin-protease complexes (SPCs) may serve a purpose. In mammals, some SPCs associate with cell surface low-density lipoprotein receptor-related proteins [Cao et al., 2006; Jensen et al., 1997]. The complexes are then engulfed by certain cells, where they trigger cell signaling. This could be another regulatory mechanism of protease activity [Cao et al., 2006; Jensen et al., 1997]. In *Drosophila*, a serpin named Necrotic form SPC

with its target protease and the complex undergoes endocytosis mediated by lipophorin receptor-1 (LpR1) [Soukup et al., 2009].

2.6 Homologs of *M. sexta* serpin10

2.6.1 *Drosophila* serpin-28D

Among 29 serpin genes found in the *Drosophila* genome, serpin-28D was reported to play roles in innate immunity and development [Schefer et al., 2008]. RT-PCR showed serpin-28D is injury inducible and mainly expressed by crystal cells. Compared to the wild type larvae, serpin-28D mutant presents stronger melanization reaction at wound site, suggesting its role in regulating injury-related PO activity. Serpin-28D RNAi knockdown flies show low PO availability and morphologically abnormal pigmentation. It is believed that the exhaustion of PO in hemolymph leads to its low availability. The serpin-28D knockdowns had low pupal viability due to ectopic melanization on trachea. As the function of serpin-28D was not affected by the MP2, Spn27A or BC mutations, its target enzyme or regulatory mechanism is unclear [Schefer et al., 2008].

2.6.2 *Anopheles gambiae* serpin6

The functional analysis of *A. gambiae* serpin6 in mosquitoes indicated that *Plasmodium* sporozoites could induce its expression in the salivary gland, whereas *Plasmodium* ookinetes induce its expression in midgut epithelial cells and hemocytes. *E. coli* invasion could induce its expression in all the tissues above. Serpin-6 is believed to be involved in parasite killing in *A. stephensi* and parasite clearance in *A. gambia*e [Abraham et al., 2005; Pinto et al., 2008].

2.6.3 *M. sexta* serpins

M. sexta is one of the insects whose serpins have been extensively studied. The serpin-1 is actually a mixture of twelve proteins with different carboxyl-terminal segments encoded by alternative exons. The variable sequences include the reactive site loop that determines the inhibitory selectivity [Jiang and Kanost, 1997]. Serpin-2 is an inducible protein expressed in certain hemocytes [Gan et al., 2001]. Serpin-3 directly inhibits PAPs [Zhu et al., 2003]. Serpin-4 inhibits HP21, HP1 and HP6 by forming covalent complexes with these proteases. Serpin-5, 58% similar to serpin-4, also inhibits HP1 and HP6. HP6 activates HP8 and PAP1 [Tong et al., 2005; Tong and Kanost, 2005]. Serpin-6 inhibits PAP3 and HP8 [Zou and Jiang, 2005], and HP8 activates spätzle, Toll, and AMP production [An et al., 2009; Zou and Jiang 2005]. Although serpin-4, -5, and -6 inhibit different target proteases, they all directly or indirectly control proPO activation. This kind of redundancy is consistent with the importance of proPO pathway.

2.7 LC/MS/MS Orbitrap peptide analysis

The use of mass spectrometry has improved the efficacy, sensitivity, and accuracy of identification and analysis of proteins. The newly developed instrumentation, software and database management have enhanced our ability and understanding in identification and quantification. The proteomics brings us the benefits in both scientific research and medical applications [Wysocki et al., 2005; Kuntumalla et al., 2009; Hu et al., 2009].

CHAPTER III

METHODOLOGY

Objective 1: Determination of the antimicrobial activity of reactive intermediates generated by phenoloxidase (PO)

1. Chemicals, proteins, and microbial strains – Dopamine, L-dopa, 1-phenyl-2-thiourea (PTU) and tyramine were purchased from Sigma. N-acetyldopamine (NADA) and N-β-alanyldopamine (NBAD) were generously provided by Dr. Michael Kanost in the Department of Biochemistry at Kansas State University. DHI, or 5,6-dihydrooxindole, was supplied by Chemical Synthesis and Drug Supply Program at National Institute of Mental Health. *M. sexta* proPO was purified from hemolymph of the 5th instar larvae according to Jiang et al. (1997). *M. sexta* PAP-3, SPH-1 and SPH-2 were isolated from plasma of the bar-stage wandering larvae as described before [Jiang et al., 2003; Wang and Jiang, 2004a]. *E. coli* Xl1-blue strain (Stratagene) was transformed with plasmid pGB5 [Bloemberg et al., 1989], a kind gift from Dr. O'Toole in Department of Microbiology and Immunology at Dartmouth Medical University. *Bacillus cereus, Bacillus subtilis, Klebsiella pneumoniae, Micrococcus luteus, Pseudomonas aeruginosa, Saccharomyces cerevisiae, Salmonella typhimurium*, and *Staphylococcus aureus* were obtained from Department of Microbiology at Oklahoma State University. *Beauveria bassiana* and *Candida albicans* were kindly provided by Drs. Stephen Marek and Guo-

long Zhang at Oklahoma State University. Most of them were reported to trigger insect immune responses, as pathogens or carried by insects [Zou et al., 2007; Wilson et al., 1999; Gulii et al., 2009; Li et al., 2001; Hillyer et al., 2004; Kuzina et al., 2001].

2. Preparation of microbial cells – A single colony of each bacterial strain was inoculated into 4 ml Luria-Bertani (LB) medium containing appropriate antibiotics and grown at 37°C for 12 h with shaking at 225 rpm. The overnight cultures (A_{600nm} = 1~2) were collected by centrifugation at 2,500×*g* for 5 min. After careful removal of the supernatant, the cell pellet was resuspended in sterile phosphate buffered saline (pH 7.4, 10 mM sodium phosphate, 150 mM NaCl) to a final A_{600nm} of 1.0. *B. bassiana, P. pastoris, C. albicans* and budding yeast *S. cerevisiae* was cultured in YEPD medium at 28°C for 16 h with shaking (260 rpm). The cells were harvested by centrifugation and resuspended in the same buffer (A_{600nm} = 1.0).

3. PPO activation and substrate selection – Purified PPO (0.2 mg/ml, 2 μl), PAP3 (30 ng/ml, 2 μl), and SPHs (30 ng/ml, 2 μl) were added to 14 μl, 20 mM Tris-HCl, pH 7.5 in a microplate well. After incubation on ice for 1 h, the activation mixture was reacted with 150 μl, 50 mM sodium phosphate (pH 6.5) containing 2 mM tyramine, L-dopa, dopamine, NADA, or NBAD. Quinone and melanochrome formation was measured every 15 s for 5 min at 350 nm and 470 nm, respectively, using a Versamax^{TM} microplate reader (Molecular Devices).

4. Effect of dopamine-derived compounds on the growth of microbial cells – Resuspended *E. coli, B. subtilis* or *P. pastoris* cells (5.0 μl) were separately added to 20 μl proPO activation mixture and 150 μl dopamine solution. Negative controls were: buffer mixed with dopamine, PTU, or activation mixture alone, as well as dopamine

solution mixed with heat- or PTU-treated activation mixture. After the cells were incubated for 1.5 h at room temperature, 120 μl of the samples were inoculated into 4.0 ml medium and grown at 37°C with shaking. For the bacteria, A_{600nm} readings were taken at 1~2 h intervals for 4~10 h, whereas for the yeast, absorbance was read every 4 h for one day.

5. Phase-contrast and fluorescence microscopy – After *E. coli* and *B. subtilis* were treated with dopamine in the presence of absence of PO for 1 h, 10 μl of the reaction and control mixtures were added onto a glass slide. The bacterial cells were observed and photographed with phase contrast or fluorescence optics under an Olympus BH-2 microscope.

6. Bacterial colony counting – After being treated by dopamine with or without PO for 16 h, *E. coli* and *B. subtilis* cells in the reaction and control were diluted with sterile PBS to 10^{-1}, 10^{-2}, 10^{-3}, 10^{-4}, 10^{-5}, 10^{-6} and 10^{-7}. Diluted cell suspensions (20 μl each) were spread to marked areas (1 cm x 1 cm) on LB agar plates. The dried plates were inversed and incubated at 37°C for 12 h (*B. subtilis*) or 18 h (*E. coli*). Additionally, the treated and control bacteria were sonicated in a water bath for 2.5 min to disperse cell aggregates. After aggregate dissociation was confirmed by microscopy, serial dilution and colony growth were performed as described above for *B. subtilis* or *E. coli*. The same experiment was carried out to test the survival of the other bacteria: *B. cereus, M. luteus, S. aureus, K. pneumoniae, P. aeruginosa*, and *S. typhimurium*. Dependent on their growth rates, the plates were incubated for 6 to 48 h so that colonies had a proper size for counting.

7. Cytotoxicity of DHI – The *Sf*9 insect cells were incubated with DHI at different concentrations in phosphate buffer (0.5 mM, pH 6.0) for 4 h. Morphological change of

the cells were observed in six-well plates by microscopy. After washing cells in 96-well plate with the buffer, 200 µl fresh medium and 20 µl 5 mg/mL 3-(4,5-dimethylthiazol-2-yl)-2,5-diphenyltetrazolium bromide (MTT) were added to each well and incubated for 4 h. The mixture of MTT and medium was removed, the cells were washed with PB, 150 µL DMSO was added to the wells, and the plate was shaken on a shaker to allow thorough dissolution of MTT. A_{492nm} readings, which correlate with cell viability was taken and plotted against DHI concentrations. The sample treated with 0.5 mM DHI at 27°C for 6 h were stained by 300 nM 4',6-diamidino-2-phenylindole (DAPI) and observed under a fluorescence microscope, Olympus BX-51.

The control and DHI-treated cells (0.5 mM at 27°C for 6 h) were washed by PBS twice and staining buffer once. Then the samples were stained with Evans blue, propidium iodide (PI) or fluorescein-labeled Annexin V for 15 min and observed by fluorescence microscopy at an exposure time of 100 ms. The staining kit, Annexin V FITC Apoptosis Detection Kit I, was purchased from BD Bioscience. Vitality of the stained cells was analyzed on a BD FACS Calibur flowcytometer. For actin staining, the cells treated overnight were washed by Annexin V staining buffer and stained with Oregan green 448 or Alexa 568 conjugated to phalloidin (Invitrogen). For cell membrane and dead cell staining, SYTO9 and PI (Molecular Probes) were used and images were obtained on the Olympus BX-51. Since the images were not used for quantification, most of them had been processed with brightness and contrast adjustment or Auto Levels in Photoshop.

The *Sf*9 cells were treated with 0.25 mM DHI overnight. Treated and control cells were washed with PBS once and resuspended in PBS. Two mL of cells were collected by

centrifugation at 1000 rpm for total DNA extraction. Lysis buffer (1% N-lauroyl sarcosine, 12.1 g Tris, 5.8 g NaCl, 17.2 mL 0.5 M EDTA, pH 8.5 in l liter) (700 μL) was added to the cells and vortexed for 1 min. Phenol:chloroform:isoamyialcohol = 25:24:1 (700 μL) was mixed with the suspension thoroughly and gently. After 5 min centrifugation at 14000 rpm, the upper layer was collected and mixed gently with the same volume of cold chloroform. After 2 min centrifugation at 14000 rpm, the aqueous phase was supplemented with 1/10 volume of 3 M sodium acetate, pH 4.8. Equal volume of cold isopropanol was mixed with the solution gently. The precipitate was collected by a pipet tip. If the amount of the precipitate is too little, collect it by centrifugation at 14000 rpm for 15 min. After washing with cold 75% ethanol, the pellet was air-dried for 2~3 h and then dissolved in TE buffer. Following RNase treatment, 5 μL of DNA samples with 2 μL loading dye were analyzed by 1% agarose gel electrophoresis.

8. Antiviral activity of DHI – To test antiviral activity of DHI, a recombinant baculovirus expressing *Schizaphis graminum* acetylcholinesterase-1 (*Sg*AChE1) [Zhao et al., 2010], was incubated with 1 μM DHI or medium at room temperature for 4 h. The treated and control baculovirus were used to infect *Spodoptera frugiperda Sf*9 insect cells (10^5 cells/ml) on a 6-well plate at 28°C for 84 h. Acetylcholinesterase activity in the culture medium was measured using the modified Ellman method [Ellman et al., 1961; Zhao et al., 2010]. The recombinant protein inside cells was examined by immunohistochemical detection using monoclonal anti-$(His)_5$ antibody and fluorescein-labeled goat-anti-mouse secondary antibody. Lambda bacteriophage was tested by incubating with DHI at different concentrations for 2.5 h at room temperature. After infecting the same number of *E. coli* Xl1-blue cells, the phage-bacteria mixtures were mixed with melted 0.8%

agarose in NZYDT and plated on pre-warmed LBB plates. Following overnight incubation at 37°C, plaque numbers were counted to calculate the phage titers for plotting against DHI concentrations.

9. Possible mechanism of DHI toxicity – The *Nco*I-*Hin*dIII digested H_6pQE60 DNA was recovered and purified from 1% agarose gel (Qiagen). The plasmid or enzyme-digested DNA and DHI at different concentrations (2.0, 1.0, 0.2, 0.1, 0.02, and 0 mM) were mixed 1:1 (v/v). After being incubated at room temperature for 1.5 h or overnight, treated DNA samples were separated by 1% agarose gel electrophoresis.

The purified recombinant *Sg*AChE1 was incubated with same volume of 2.0 mM DHI or buffer overnight at room temperature. Residual activity in the control and DHI-treated sample were measured as described above.

Bovine serum albumin (BSA, 500 mg/mL) was mixed with same volume of DHI solution at different concentration (2.0, 1.0, 0.5, 0.25 and 0.125 mM). Control sample was mixed with 50 mM phosphate buffer (PB), pH6.5. The samples were subjected to 10% native polyacrylamide gel electrophoresis (PAGE), non-reducing and reducing SDS-PAGE. Sizes of the control and treated samples were analyzed on a Zetasizer (Malvern).

Objective 2: Expression and functional characterization of *M. sexta* serpin-10

1. Phylogenetic analysis of *M. sexta* serpin-10 and its homologs – To confirm classification as serpins, the protein sequences were scanned for domain features using CDART [Geer et al., 2002], PROSITE, and SMART [Schultz et al., 1998, Ponting et al., 1999; Letunic et al., 2009]. Signal peptides were predicted using SignalP3.0. Complete serpin domains were aligned using ClustalX 1.83 [Thompson et al., 1994; Thompson et

al., 1997]. Phylograms using neighbor-joining algorithm were displayed through Treeview [Page, 2002]. A Blosum 30 matrix, a gap penalty of 10 and an extension gap penalty of 0.05 were selected for the multiple sequence alignment.

2. Construction of serpin10/pMFH6 – For PCR amplification of the cDNA fragment, each 50 µl-reaction contained 5 ng full-length serpin-10 cDNA in pBluescript from *M. sexta* cDNA library, 20 pmol of each primer (j141: 5'-CCCATGGGAATTCAAGATGA ACAATAC and j142: 5'-AAGCTTACTCGAGTCCTTTTGTGGGATCGAA) and Advantage cDNA polymerase mix (5 U). The gel-purified PCR products were cloned into pGEM-T and plasmids from the resulting transformants were sequenced entirely to ensure error-free inserts. The cDNA segments, retrieved by digestion with *Eco*RI and *Xho*I, were inserted to the same sites of pMFH6 [Lu and Jiang, 2008] to generate plasmid serpin10/pMFH6. The modified Bac-to-Bac vector allows recombinant proteins synthesized under the control of polyhedrin promoter, secreted into media using the honeybee mellitin signal peptide, and purified on a Ni-NTA column via the carboxyl-terminal hexahistidine tag.

3. Construction of recombinant baculovirus for expressing $(His)_6$-tagged serpin-10 – *In vivo* transposition of the expression cassette in serpin10/pMFH6, selection of bacterial colonies carrying recombinant bacmids, and isolation of bacmid DNA were performed according to the manufacturer's protocols (Life Technologies, Inc). The initial viral stock was obtained by transfecting *Sf*21 cells with a bacmid DNA-CellFECTIN mixture, and its titer improved through serial infections.

4. Expression and purification of *M. sexta* serpin-10 from insect cells – *Sf*9 cells (3.0×10^6 cells/ml), 1L SF-900III serum-free medium (Invitrogen) were infected by the viral stock

at a multiplicity of infection of 10 and grown at 24°C for 96 h with agitation at 100 rpm. The conditioned medium was harvested by centrifugation at 6000 rpm for 10 min, diluted with 0.1 M sodium phosphate buffer (pH 6.3), and mixed with dextran sulfate-Sepharose (100 ml) for 1 h at 4°C. After washing with the buffer, bound proteins were eluted by 1.2 M NaCl in the phosphate buffer. After immunoblot analysis using anti-His antibodies (Bio-Rad), pooled serpin-10 fractions were mixed with 10 mL Ni-NTA beads overnight at 4°C and loaded onto a column. After washing with 20 ml 30 mM imidazole, in phosphate buffered saline, pH 7.5, serpin-10 was eluted with 300 mM imidazole in the same buffer. Protein concentrations were determined by Coomassie Plus Protein Assay (Pierce) in each purification step. The purified serpin-10 (500 μg) was used as antigen for raising a rabbit polyclonal antiserum (Cocalico Biological Inc.).

5. Reverse transcription (RT)-PCR analysis of *M. sexta* serpin-10 mRNA levels – Total RNA was extracted from hemocytes and fat body of naive and bacteria-injected *M. sexta* 5th instar larvae [Zhu et al., 2003]. cDNA was synthesized using total RNA as template, oligo-dT as primer, and reverse-transcriptase (Invitrogen). Equal amount of cDNA from control and induced insects were used as templates for semi-quantitative RT-PCR under nonsaturating conditions. The primer pairs for ribosomal protein S3 (internal control) and serpin-10 are j037-j038 (5'-CATGATCCACTCCGGTGACC and 5'-CGGGAGCATGA TTTTGACCTTAA) and j125-j126 (5'-TGAACATGTAGAATGGGGAGTC and 5'-CG TCGGCGAGGCTCTCAGTG), respectively. The PCR products were resolved by 1.5% argrose gel electrophoresis to detect the relative transcription levels of serpin-10 in the samples from different tissues (nerve, salivary gland, trachea, Malpighian tubule, midgut, integument, muscle cDNA), fat body of different developmental stages (4th instar days 0

to 5; 5th instar days 0 to 6; wandering stage days 1 to 6, pupae at early, middle, and late stages; adult) and hemocytes with fat body of different immune states at 0, 1.5, 3.0, 4.5, 6.0, … 21, 22.5, and 24 h after injection.

6. Immunoblot analysis of *M. sexta* serpin-10 and associated complex with hemolymph proteins – Cell-free hemolymph from naïve and bacteria-injected *M. sexta* larvae was incubated with saline, Gram-negative or Gram-positive bacteria and then treated with SDS-sample buffer. After 10% SDS-PAGE and electrotransfer, Western blot analysis was performed using 1:2000 diluted serpin10 antiserum and 1:2000 alkaline phosphatase (AP)-linked secondary antibody. The expression levels of serpin-10 in plasma samples before and after the immune challenge were examined. The plasma containing the SPC was used for affinity purification of the complex and associated hemolymph proteins.

7. Isolation of immune protein complex containing *M. sexta* serpin-10 – Hemolymph (60 mL from 5th instar *M. sexta* larvae) was diluted with 120 ml anti-coagulant saline solution (4 mM NaCl, 40 mM KCl, 8 nM EDTA, 9.5 mM citric acid, 27 mM sodium citrate, 5% sucrose, 0.1% polyvinylpyrollidone, 1.7 mM PIPES and 1 mM PTU), activated with *M. luteus* or *E. coli* (1 μg/μL at room temperature for 30 min). Ammonium sulfate (AS) was added to reach a final saturation of 60%. After incubated at 4°C for 2 h, the hemolymph mixture was separated by centrifugation at 12000 rpm for 30 min. The pellet was collected, dissolved in hydroxyapatite (HT) buffer-A (10 mM phosphate buffer, pH 6.8, 500 mM NaCl, 0.5 mM benzamidine), and dialyzed against the same buffer. After clarification by centrifugation at 12000 rpm for 30 min, the supernatant (about 40 mL) was collected and loaded onto a 40 mL HT column (0.4 ml/min). After washing with 50 mL HT-A buffer, the proteins were eluted by 80 mL HT-A and 80 mL HT-B (100 mM

phosphate buffer, pH 6.8, 1 M NaCl, 0.5 mM benzamidine) in a linear gradient at 0.4 mL/min. After serpin-10 was detected by immunoblotting, selected fractions were pooled and dialyzed against DS-A buffer (10 mM sodium phosphate, pH 7.0). The dialyzed sample was loaded onto a 20 mL dextran sulfate (DS) column at 0.5 mL/min. After washing with 30 mL DS-A buffer, the proteins were eluted by 50 mL DS-A and 50 mL DS-B (DS-A and 1.0 M NaCl) in a linear gradient at 0.45 mL/min. Selected fractions were pooled and further separated by affinity chromatography on a serpin-10 polyclonal antibody column [Wang and Jiang, 2004b]. To isolate the complex of serpin-10 and its target serine protease, the sample from the DS column was mixed with serpin-10 antibody-coupled Protein-A Sepharose CL-4B beads at 4°C overnight. After washing with 1 M NaCl and PBS, bound proteins were eluted by 100 mM glycine-HCl, pH 2.5, 10% ethylene glycol. Fractions (500 μl each) were collected into 0.1 ml of 1 M sodium phosphate, pH 8.0. The pre-immune serum from the same rabbit was used to prepare a control column [Tong and Kanost, 2005].

8. LC/MS/MS Orbitrap peptide analysis – The elution faction sample from direct affinity chromatography and further purified sample were run on a 10% reducing SDS PAGE gel and stained with Coomassie blue. The visible bands were cut for in-gel trypsin digestion and LC/MS/MS Orbitrap (Thermo Scientific LTQ Orbitrap XL) fingerprint analysis at OSU Recombinant DNA/Protein Core Facility. The data was compared with a database of tryptic masses from *M. sexta* proteins. The search engine used Mascot, and the search results were displayed by Scaffold. The *M. sexta* database 1.0 includes the protein sequences in FASTA format directly downloaded from NCBI and contigs sequences from EST 454 sequencing project [Zou et al., 2008].

CHAPTER IV

FINDINGS

Objective 1: Determination of the antimicrobial activity of reactive intermediates generated by PO.

1. Enzymatic activity and substrate specificity of *M. sexta* PO – Pre-incubation of purified proPO, PAP-3, and SPHs generated active PO, as previously demonstrated [Wang and Jiang, 2004a]. The oxidase then converted dopamine, NADA, NBAD, and L-dopa to their corresponding quinones at comparable rates (Fig. 11).

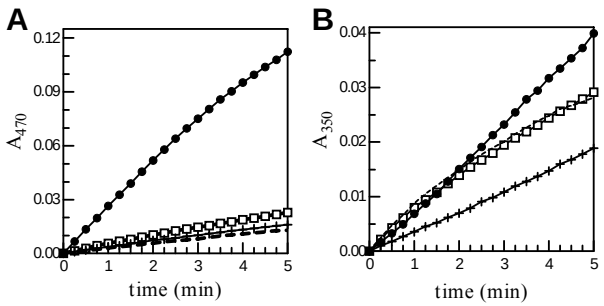

Figure 11. Progressive curves for the PO-catalyzed conversion of phenolic compounds, monitored at 470 nm (A) and 350 nm (B). Active PO generated by incubation of proPO with PAP-3 and SPHs was incubated with L-dopa (- - - - -), dopamine (● — ●), NADA (+ — +), or NBAD (□ — □).

While the quinones formed at similar rates (as indicated by absorbance increases at 350 nm), the production of melanochrome from dopamine occurred 7–10 times as fast as that from NBAD, NADA, or L-dopa. The acetyl or β-alanyl group on the side chain withdraws electrons and greatly slows down the intra-molecular nucleophilic substitution

[Aso et al., 1984].

2. Effect of PO-generated reactive intermediates on the growth of microbial cells —After PO and dopamine had been incubated with *E. coli* cells, we observed that the bacterial growth was completely blocked (Fig. 12A). This activity appeared to be concentration-dependent since the growth inhibition was incomplete when half of the PO activity was used. *E. coli* growth was not affected after the cells had been treated with the substrate or PO alone. PTU inhibition of PO abolished the growth inhibition. PTU alone did not affect the bacterial growth (Fig. 12A and B).

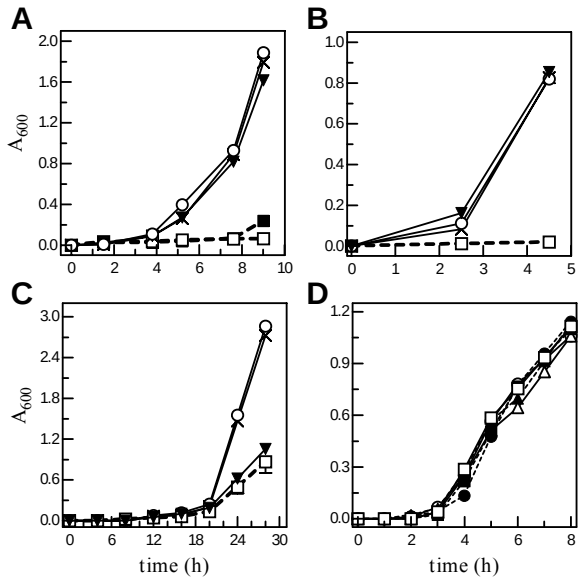

Figure 12. Effect of PO-generated reactive intermediates on the growth of *E. coli* (A), *B. subtilis* (B, D) or *P. pastoris* (C). Panels A–C: after the cell suspensions were treated with dopamine (▼ — ▼), PO (○ — ○), PTU only (Δ — Δ), dopamine with PO (□ — □), half of PO (■ — ■), or PTU-treated PO (× — ×), fresh media were added to the cells. Absorbance readings were taken from the cultures at the different intervals and plotted against time. Panel D: *B. subtilis* cells treated with NADA (□ — □), NADA and PO ((■ — ■), NBAD (Δ—Δ), NBAD and PO (▲ — ▲), L-dopa (○ — ○), L-dopa, and PO (● — ●).

These results indicated that the products resulting from the PO–dopamine reaction

were responsible for the growth inhibition. A similar effect was observed after *B. subtilis* cells had been treated with PO and dopamine. *B. subtilis* grew faster than *E. coli* and both bacteria were not affected by the presence of dopamine itself. In contrast, dopamine alone reduced the growth of *P. pastoris* (Fig. 12C). Inclusion of active PO in the substrate solution did further reduce the yeast growth, but the small effect was not statistically significant. Treating the bacterial and fungal cells with PO and another natural substrate (NADA, NBAD, or L-dopa) has little effect on their growth (Fig. 12D).

3. Microscopic detection of melanized bacterial nodules – We examined the morphology of *E. coli* and *B. subtilis* cells treated with dopamine only or dopamine and PO (Fig. 13). The control cells were smooth, transparent, and mostly isolated. On the contrary, large aggregates of the bacteria formed after incubation with the PO–dopamine reaction mixture. Parts of the cells were covered with black pigments and became rough. While movement of the control fluorescent cells was captured by photography during the exposure, PO-treated *E. coli* cells did not display such mobility even if they were not aggregated — the cell mobility was lost after the PO-dopamine treatment.

4. Bactericidal activity of PO-generated reactive intermediates – In order to test if there was any change in cell viability after the treatment, we measured the colony-forming units in the *E. coli* suspension containing dopamine only or dopamine and PO. There was a significant reduction in colony counts from 2.3×10^6 to 3.2×10^5 cfu/ml (Fig. 14A). Since cell aggregation (rather than direct killing) could also cause the decrease in CFUs, we sonicated the suspensions at a low power to disperse the aggregates. Viability of the cells reduced 35% to 1.5×10^6 cfu/ml after sonication. While large aggregates in the treated

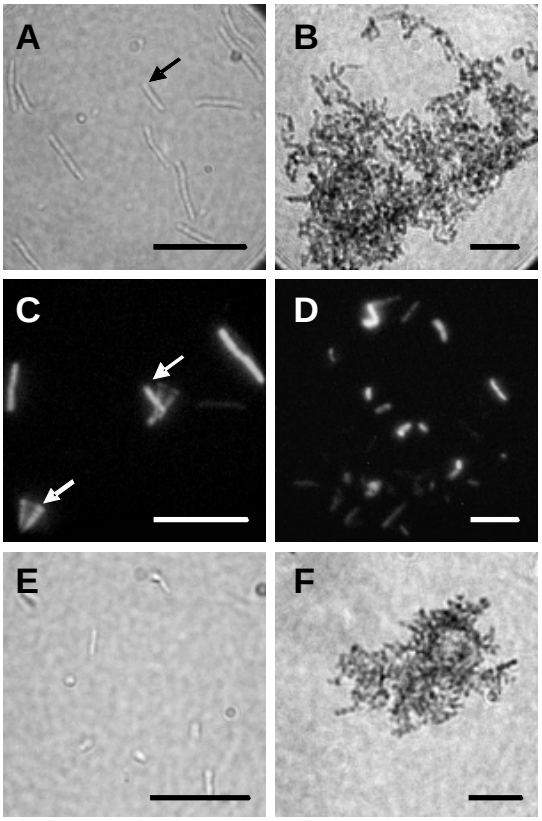

Figure 13. Morphology, mobility, and association states of the bacterial cells examined under the phase-contrast (A, B, E, and F) and fluorescence (C, D) microscope. As indicated in the Materials and Methods, *E. coli* (A–D) or *B. subtilis* (E, F) were treated with dopamine only (A, C, E) or dopamine and PO (B, D, F) at room temperature for 16 h. The suspensions were added to a glass slide and photographed with different optics. The length of scale bar is equivalent to 10 μm.

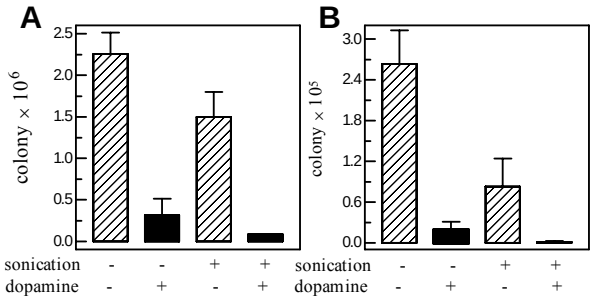

Figure 14. Effect of PO-generated reactive compounds on viability of *E. coli* (A) and *B. subtilis* (B). After the bacterial cells were treated with dopamine only or dopamine with PO at room temperature for 2 h, the suspensions were either directly diluted and grown on solid medium or sonicated before serial dilution and culturing. The colony counts (cfu/ml) were plotted in the bar graph as mean ± SD (n=4).

Table 1. Bactericidal activity of reactive compounds generated by *M. sexta* PO

bacterial species	colony counts		% of control
	control	treatment	
Gram-positive			
Bacillus cereus	$5.2\pm2.3\times10^5$ (n=4)	$1.4\pm2.4\times10^3$ (n=4)	0.27
Bacillus subtilis	$9.8\pm8.2\times10^4$ (n=4)	$1.2\pm2.4\times10^3$ (n=4)	1.2
Micrococcus luteus	$5.8\pm1.6\times10^6$ (n=4)	$3.0\pm3.6\times10^6$ (n=4)	52
Staphylococcus aureus	$1.4\pm0.1\times10^6$ (n=4)	$6.8\pm1.4\times10^5$ (n=4)	48
Gram-negative			
Escherichia coli	$1.5\pm0.6\times10^6$ (n=4)	$8.6\pm3.0\times10^4$ (n=4)	5.7
Klebsiella pneumoniae	$1.8\pm1.8\times10^8$ (n=4)	$1.3\pm0.7\times10^7$ (n=4)	7.2
Pseudomonas aeruginosa	$1.3\pm0.1\times10^7$ (n=4)	$2.1\pm1.2\times10^6$ (n=4)	16
Salmonella typhimurium	$2.4\pm0.9\times10^7$ (n=6)	$9.6\pm0.9\times10^6$ (n=5)	40

Appropriate ranges of cfu/ml were determined for individual bacterial species in preliminary experiments. The results are presented as mean ± CI (α=0.05, n= 4~6) and percentage of survival.

cells were well separated after sonication (data not shown), the colony counts did not increase. On the contrary, we detected a 73% decrease to 8.6×10^4 cfu/ml — PO-dopamine treated *E. coli* cells seemed to be more susceptible to sonication. These data suggested that PO-generated reactive compounds were responsible for aggregation and death of *E. coli*. The antimicrobial activity was not limited to *E. coli*: more striking results were obtained when *B. subtilis* cells were tested (Fig. 14B). Before and after sonication, the cell mortality was determined to be 93% and 99% higher in the samples treated with PO and dopamine.

To examine specificity of this bactericidal effect, we tested other bacterial species: three Gram-positive and three Gram-negative (Table 1). *B. cereus* was most susceptible while *S. aureus* was most resistant: after PO–dopamine treatment and sonication, 99.7% and 52% of the cells died. In comparison, 60–94% of the Gram-negative bacteria were killed after the treatment.

5. Chemical nature of the bactericidal compounds – Why did dopamine greatly affect the bacterial survival (Table 1) and growth (Fig. 12, A and B) but NADA or NBAD did not (Fig. 12D)? After comparing the structural differences between dopamine and its acyl derivatives (Fig. 15), we hypothesized that dopamine quinone or its subsequent reaction products had the bactericidal activity. Since dopamine and the other plasma catecholamines were all converted to their corresponding quinones (Fig. 11), it seemed less plausible that dopamine quinone was responsible for the killing. Therefore, we tested the antimicrobial activity of DHI, a compound formed by spontaneous cyclization of dopamine quinone — NADA and NBAD quinones form DHI derivatives at a much lower rate (Aso et al., 1984).

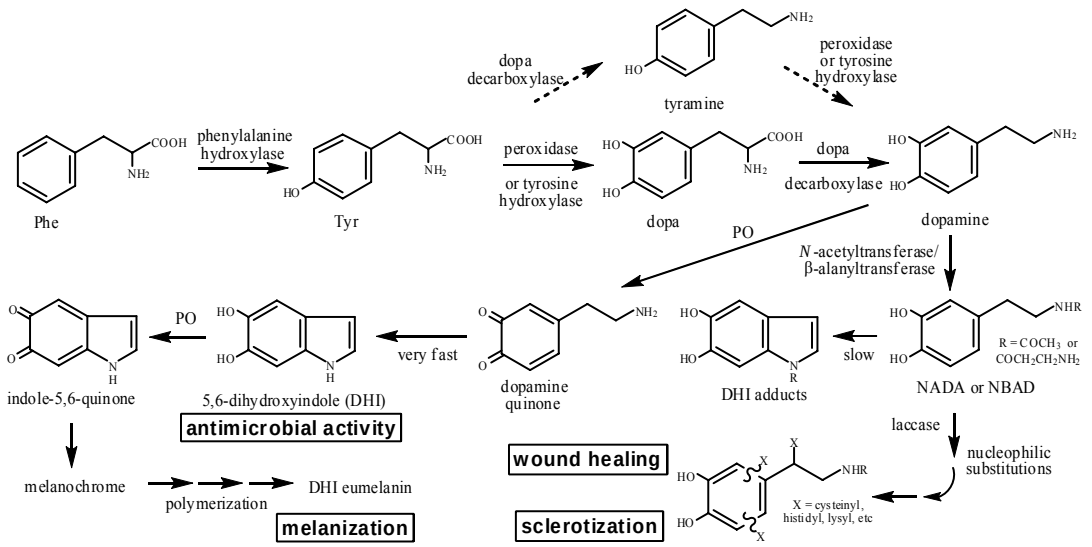

Figure 15. Mechanisms and physiological functions of PO-mediated reactions in insects and crustaceans. Tyrosinase-type POs, along with other enzymes, generates dopamine quinone which rapidly cyclizes to form DHI nonenzymatically. DHI, as well as its oxidation products, has a broad-spectrum antimicrobial activity (this work). These products spontaneously polymerize to form melanin frequently observed around wounds, pathogens, or parasites. Dopamine can also form stable derivatives through acyl transfer. Laccase-type POs then convert NADA and NBAD to oxidative intermediates for protein crosslinking during wound healing and cuticle sclerotization.

In the absence of PO, DHI spontaneously oxidizes to form indole-5,6-quinone and

melanochrome that polymerizes to become DHI eumelanin (Fig. 15). These reactions occurred at a ~30% higher rate in the presence of PO (Fig. 16A), confirming that *M. sexta* PO had a broad substrate specificity by acting on multiple steps of the quinone production and melanin formation (Hall et al., 1995; Sugumaran, 2002; Nappi and Christensen, 2005). DHI and/or its products resulted from spontaneous oxidation killed *E. coli* and *B. subtilis* more efficiently than dopamine-derived compounds — more than 99.9% of the bacteria died (Fig. 16, B and C).

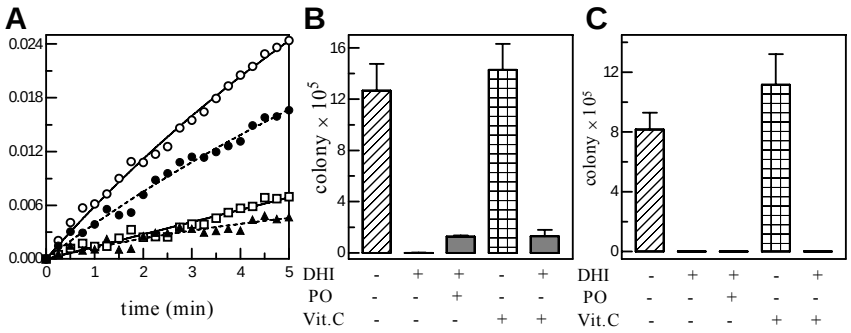

Figure 16. PO-catalyzed DHI oxidation (A) and the bactericidal activity of DHI (B, C). (A) Progressive curve. After DHI was added to PBS or active PO, absorbance was monitored at 350 and 470 nm on a plate reader. DHI and PO at 350 nm (○ — ○); DHI only at 350 nm (● — ●), DHI and PO at 470 nm (□ — □); DHI only at 470 nm (▲ — ▲). (B) *E. coli* and (C) *B. subtilis*. After the bacterial cells were treated with PBS, vitamin C, DHI, DHI+vitamin C, or DHI+PO at room temperature for 1 h, the cell suspensions were sonicated, diluted, and grown on solid LB medium. The colony counts (cfu/ml) were plotted in the bar graph as mean ± SD (n=4).

We also examined the effect of decrease or increase in the oxidation of DHI. While vitamin C itself did not affect the bacterial colony counts, its inclusion in the DHI solution slowed down the spontaneous oxidation (data not shown) and led to a 9.0% decrease in the *E. coli* mortality (Fig. 16B). To our surprise, an increase in the rate of oxidation by adding PO also gave rise to lower mortality rates (90.2% for *E. coli* and 99.8% for *B. subtilis*). These results are consistent with the observation that *B. subtilis*

cells are more susceptible to the treatment than *E. coli* are (Table 1), and further suggested that DHI was the compound that killed the bacteria. Interestingly, DHI is a catechol rather than a quinone, which has long been assumed to be cytotoxic.

6. Antifungal activity of DHI – To investigate if the minor inhibition of *P. pastoris* growth (Fig. 12C) was due to limited amount of DHI produced in the PO–dopamine reaction (and its strong cell wall), we directly treated the yeast cells with DHI and observed significant growth inhibition (Fig. 17A). Viability tests showed DHI alone had the highest fungicidal activity (92.9% mortality), and inclusion of vitamin C or PO lowered the effect (39.7% and 50.3% mortality) (Fig. 17B). We further examined the activity against other fungal species, including the entomopathogenic fungus *B. bassiana* (Fig. 17C). The mortality rates of *S. cerevisiae*, *C. albicans*, and *B. bassiana* after DHI treatment were 99.5%, 99.3%, and 90.19%, respectively.

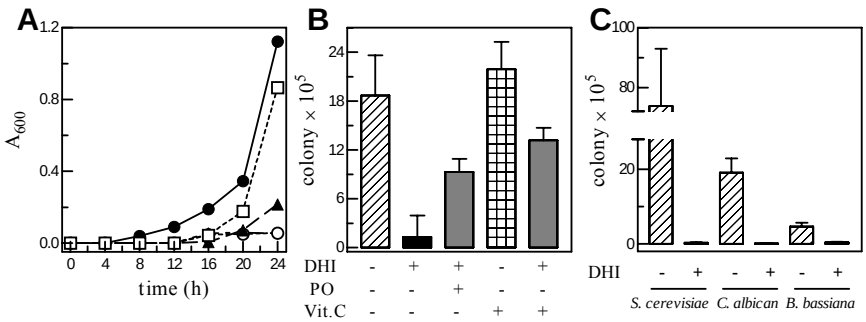

Figure 17. Effect of DHI on the survival and growth of fungi. (A) *P. pastoris* growth inhibition: vitamin C (● — ●); PBS (□ — □); DHI+vitamin C (▲ — ▲); DHI+PO (○ — ○); DHI only (♦ — ♦). (B) Killing of *P. pastoris*: after the yeast cells were treated with buffer, DHI, vitamin C, DHI+vitamin C, or DHI+PO at room temperature for 1 h, the cell suspensions were diluted and grown on solid YEPD medium prior to colony counting. (C) Antifungal activity against *S. cerevisiae*, *C. albicans*, and *B. bassiana*. Following buffer or DHI treatment, the fungal cells were sonicated, diluted, and grown on the solid medium. The colony counts (cfu/ml) were plotted in the bar graph as mean ± SD (n=4).

7. Antiviral activity of DHI – To facilitate the measurement of possible virucidal activity

of DHI on baculovirus, we took advantage of an existing recombinant virus that secreted *S. graminum* acetylcholinesterase-1 into the medium (Zhao et al., 2010). After treating the viral stock with 1.25 mM DHI or buffer for 3 h, we infected *Sf*9 cells with the treated samples for 72 h and determined the enzymatic activity in the conditioned media. As compared with the control, only about 3% of the activity was present in the culture containing DHI-treated virus (Fig. 18A), suggesting over 97% of the viruses were killed during DHI treatment. We did not observe any sign of viral infection in the *Sf*9 cells. In contrast to the control cells, no fluorescence signal was detected in cells infected with the DHI-treated viruses (Fig. 18B).

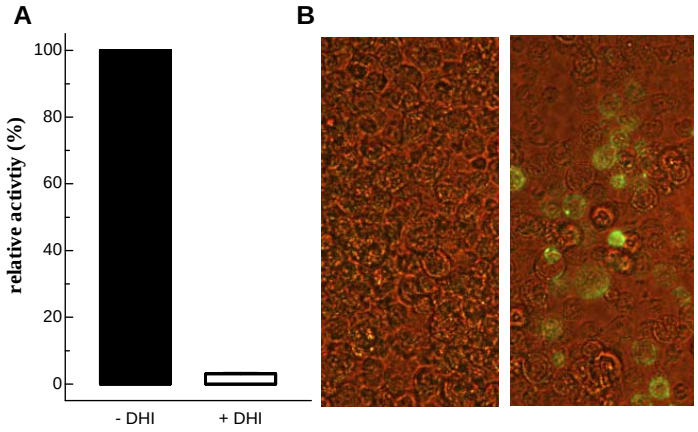

Figure 18. The virucidal activity of DHI against baculovirus. (A) Acetylcholinesterase activity in the conditioned media of Sf9 cell cultures infected with the baculovirus incubated with 1.25 mM DHI (*open bar*) or buffer (*close bar*). (B) Immunofluorescence detection of the recombinant protein inside the treated (left panel) and control (right panel) cells.

To directly quantify viral titers, we selected lambda bacteriophage to test whether treatment with DHI leads to phage death in a concentration-dependent manner. As shown in Fig. 19A, almost all the phages were killed by 1 mM DHI after 4 h incubation. Decrease in DHI concentration was accompanied by a viability increase, and the highest plaque count was found in the control. LC_{50} of DHI was 5.61 ± 2.21 μM for lambda

phage (Fig. 19B).

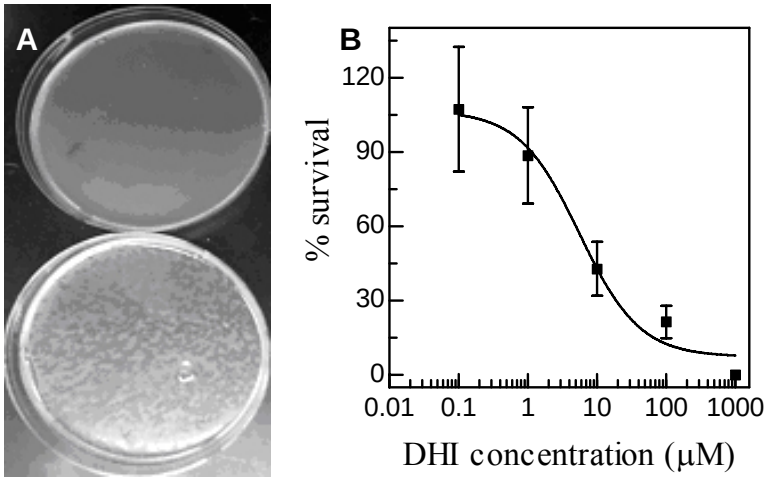

Figure 19. The antiviral activity of DHI against lambda phages. (A) Plaques formed on the lawn of *E. coli* Xl1-Blue infected with lambda phages incubated with 1.0 mM DHI (*top panel*) or buffer (bottom *panel*). (B) Concentration-dependent killing of the bacteriophages. Sigmoidal dose-response curve is used to fit the experimental data (mean ± SEM, n = 3).

8. Cytotoxicity of DHI to insect cells – As a powerful weapon against invading pathogens and parasites, PO-generated reactive chemicals may also cause damage to host tissues and cells. To test the hypothesis, we examined possible cytotoxic effect of DHI to *Sf*9 cells. Buffer-treated cells took up more MTT which, upon DMSO treatment, was released into medium and gave rise to the highest absorbance reading at 492 nm. In contrast, as DHI concentration increased, fewer live cells were left to take up the dye, which led to a concentration-dependant reduction in OD_{492} (Fig. 20A). Flowcytometry distinguished the dead cells population by detecting PI signal from DHI-treated *Sf*9 cells samples in SF900III insect cell medium, and the population of surviving cells decreased with the increasing of DHI concentration (Fig. 20B). And the toxicity of DHI to *Sf*9 cells became lower, when the treatment is in cell medium. The LC_{50} of DHI to *Sf*9 cells in buffer or in

cell medium was estimated to be 20.3 ± 1.2 μM and 131.8 ± 1.1 μM, respectively. Interestingly, the nuclei of DHI-treated cells were released into the medium whereas the remaining parts of these cells appeared to be intact and properly shaped (Fig. 21).

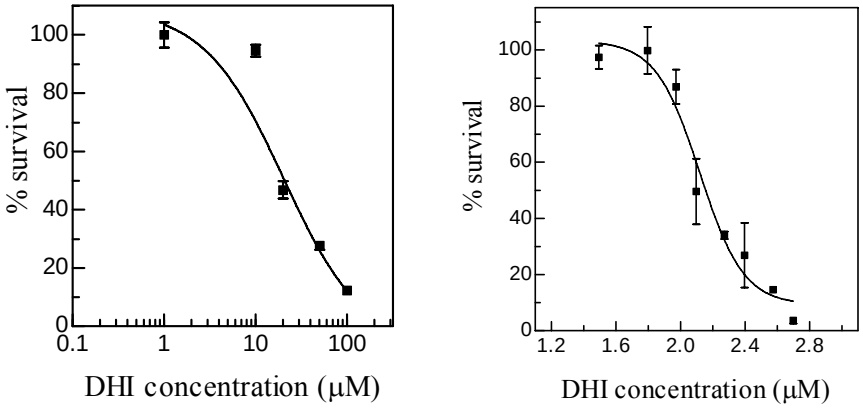

Figure 20. Concentration-dependent killing of *Sf*9 cells. *Left panel:* Cells were treated by 0, 1, 10, 20, 50, 100 μM DHI in 50 mM sodium phosphate (pH 6.5). OD_{495} readings of the DHI-treated cells were normalized against that of the control cells (100%). *Right* panel: Cells were treated by 0, 31, 63, 94, 125, 188, 250, 375 and 500 μM DHI in SF900III medium. Survival of *Sf*9 cells was quantified by flowcytometry and normalized against that of the control (100%). Curve was generated by Prism3 sigmoidal dose-response, with error bars as SEM.

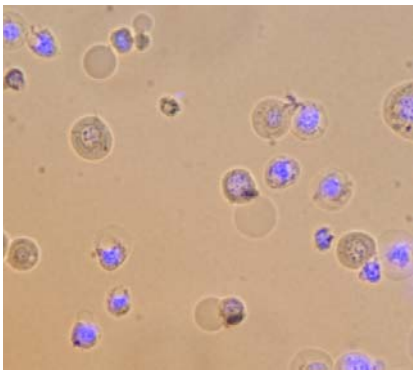

Figure 21. Cytotoxicity of DHI to *Sf*9 cells. DHI-treated *Sf*9 cells under bright field and fluorescence microscope, with DAPI-stained nuclei showing blue.

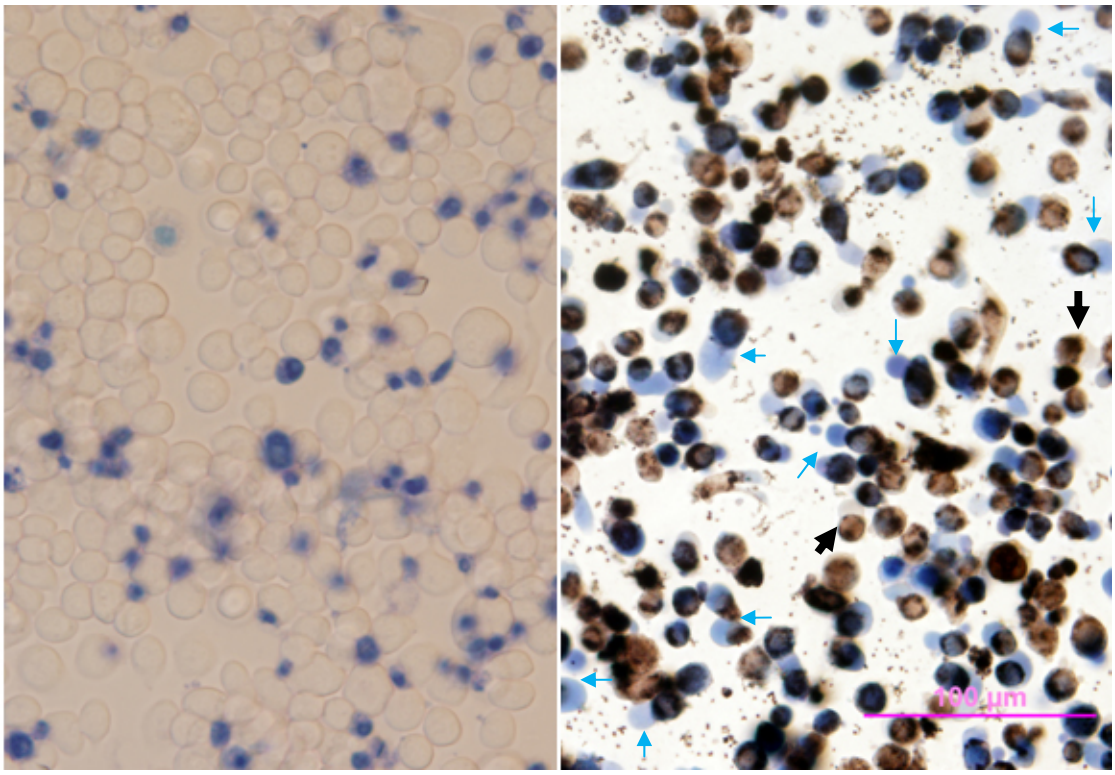

Figure 22. Evans blue-stained control (*left panel*) and DHI-treated (*right panel*) *Sf*9 cells under bright field (image processed with Auto Levels in Photoshop). Blue and black arrows indicate cell membrane structures that Evans Blue-positive and -negative, respectively.

Evans Blue is a membrane impermeable dye used to stain proteins in dead cells, as living cells exclude it. In the control *Sf*9 cells incubated with medium only, we found a small portion of them were dead (Fig. 22, *left* panel). In contrast, most of the DHI-treated cells were stained by Evans Blue. Cellular contents, colored brown due to DHI eumelanin, were partially or completely released into the medium, leaving behind membranous sacs filled with the blue dye (Fig. 22, *right* panel). Plasma membrane of a few other cells (marked by black arrows) remained intact: even though their contents had moved to one side, the empty space left behind was translucent and dye-free.

To test if DHI-treated cells were undergoing apoptosis and to further examine the membrane integrity, we employed Annexin V to specifically bind phosphatidylserine, a

component of inner layer of the plasma membrane in normal cells. At an early stage of apoptosis, plasma membrane exposes phosphatidylserine on the outer surface without membrane destruction. By combining FITC-labeled Annexin V and PI (a membrane-impermeable DNA dye), we could distinguish early-stage apoptotic cells from late-stage apoptotic or dead cells. The early-stage apoptotic cells were Annexin V positive and PI negative, whereas the latter two were Annexin V and PI double positive. In the control, most of the *Sf*9 cells were colorless and transparent under bright field (Fig. 23).

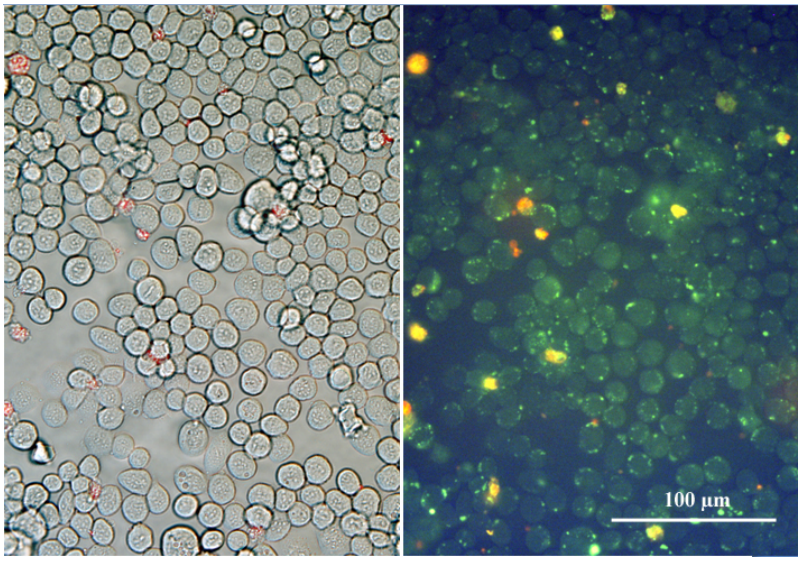

Figure 23. FITC-Annexin V- and PI-stained control *Sf*9 cells under bright field with fluorescence (left) and under dark field with fluorescence (right) (Image processed with Auto Levels in Photoshop).

Little FITC signal was observed under fluorescence, indicating most cells were healthy. Only a small fraction of cells were dead and, thus, stained by PI which emitted red light. However, in the DHI-treated sample, a lot more cells underwent polarization and rupture that released cellular contents (Fig. 24). A small portion of cells (*e.g.* cells surrounding the white triangle) were healthy and, thus, not stained by either dye. Other cells became Annexin positive (bright green cells) and then polarized (as indicated by white arrows),

but not emitting red light. The late-stage apoptotic or dead cells were generally small in size and stained by Annexin V and PI at various levels. The released cellular contents, detected as melanized bodies, were not labeled by either stain.

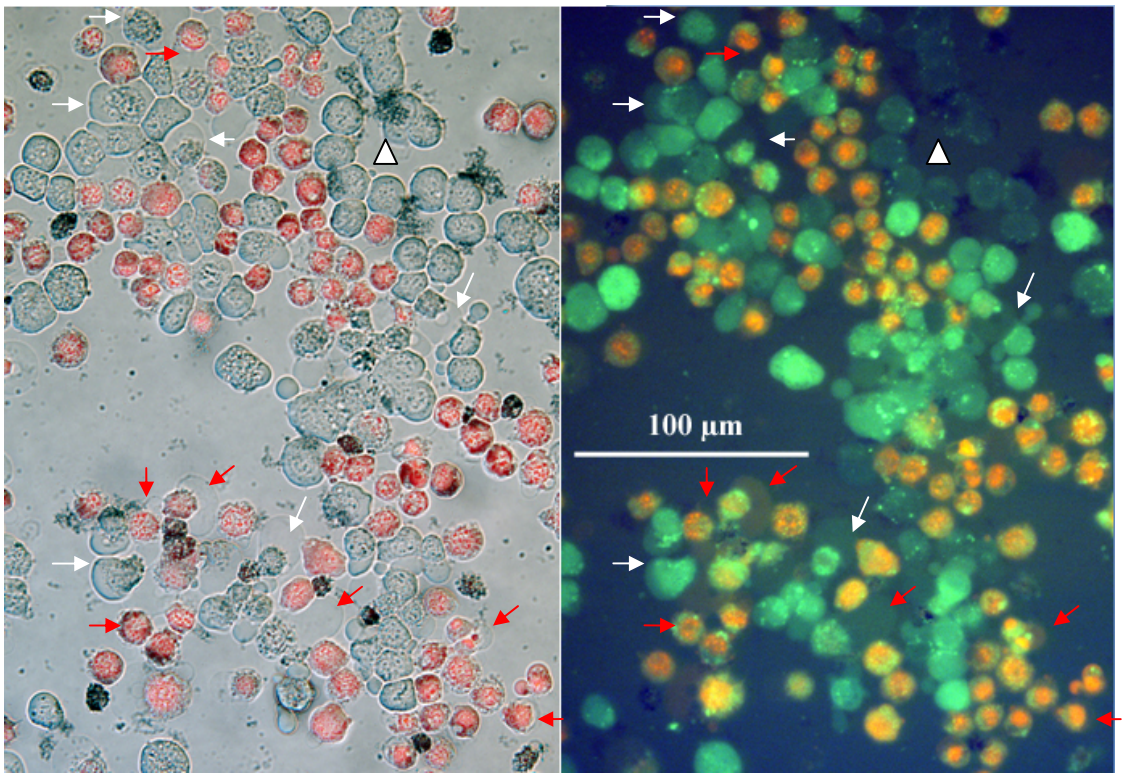

Figure 24. FITC-Annexin V- and PI-stained *Sf*9 cells (treated with 0.5 mM DHI) under bright field with fluorescence (left) and under dark field with fluorescence (right). White arrows point at Annexin V positive and PI negative cells, whose contents were polarized and about to be released. Red arrows point at PI positive cells, which are releasing cell contents, and most of the cell contents are also AnnexinV positive. The image has been processed with Auto Levels by Photoshop.

To confirm the apoptosis, we extracted DNA from *Sf*9 cells treated with buffer only or with 0.25 mM DHI overnight and separated the samples by 1.0% agarose gel electrophoresis. The control DNA did not run much into the gel, whereas a portion of the test sample migrated as a series of bands at approximately 180 bp, 360 bp, 540 bp, 720

bp, and so on (Fig. 25). The fragmentation of genomic DNA down to ~180 bp units is a characteristic feature of apoptosis.

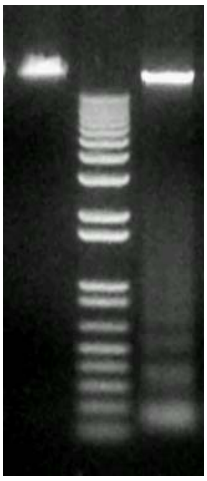

Figure 25. 1.0% Agarose gel electrophoretic analysis of genomic DNA from *Sf*9 cells incubated overnight with buffer or 0.25 mM DHI. *Left* lane, DNA of the control cells; *middle* lane, 1 kb DNA size markers (12, 11, 10, 9, 8, 7, 6, 5, 4, 3, 2, 1.6, 1, 0.85, 0.65, 0.5, 0.4, 0.3, 0.2, 0.1 kb); right lane: DNA of the DHI-treated *Sf*9 cells.

9. DHI mediated DNA and protein polymerization – To explore mechanism for the antimicrobial activity and cytotoxicity of DHI, we treated circular and linearized plasmid DNA samples with DHI at various amounts. Electrophoretic analysis indicated that the amount of original-sized DNA decreased as DHI concentration increased (Fig. 26). There was a concurrent increase in DNA species with larger sizes, suggesting that DHI caused the DNA molecules to form high molecular weight aggregates. The longer the treatment, the more aggregates formed – after overnight treatment, plasmid and linear DNA treated with 0.5 and 1.0 mM DHI disappeared at the original sizes.

We also tested a possible effect of DHI on two proteins, *Sg*AChE1 and BSA. After incubating purified recombinant *Sg*AChE1 with DHI, we detected a loss of nearly

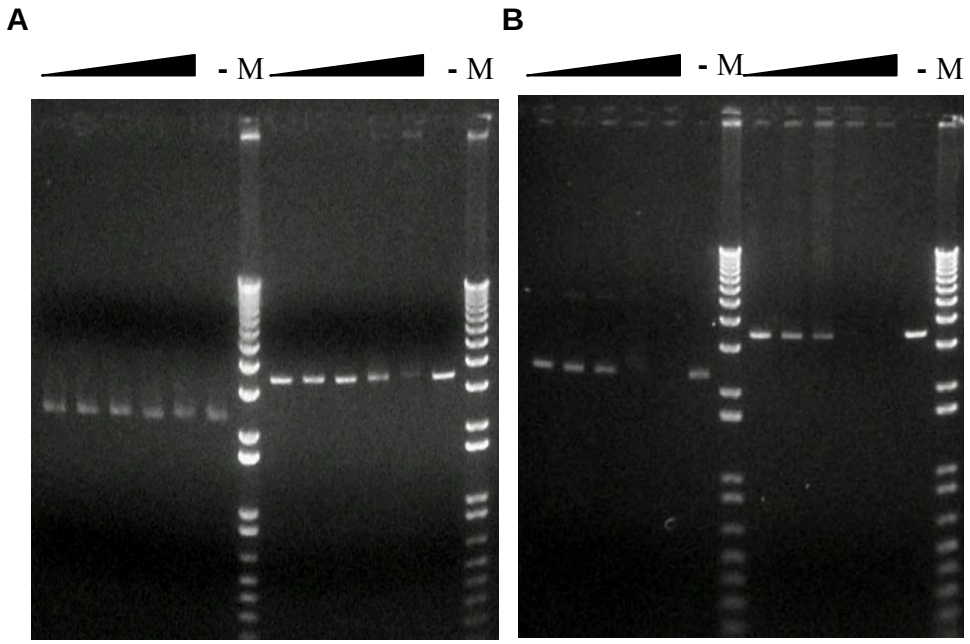

Figure 26. Effect of DHI treatment on circular and linear plasmid DNA. A) 1.5 h; B) overnight. *Left* side, circular DNA treated with 0.01, 0.05, 0.1, 0.5, 1.0 mM DHI; *right* side, plasmid digested with *Nco*I and *Hin*dIII treated with DHI at the same concentrations. "–": negative control of untreated DNA; "M": 1 kb DNA size markers.

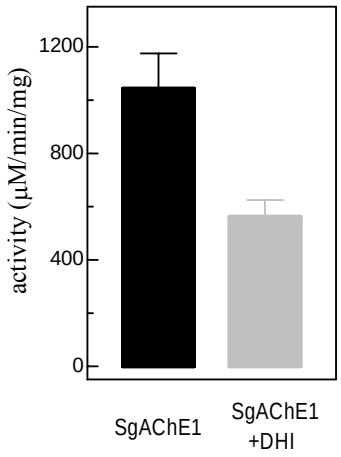

Figure 27. Aacetylcholinesterase activity of control and DHI-treated *Sg*AChE1.

50% of its activity (Fig. 27), in comparison with the control. In the other experiment, DHI-treated BSA samples showed a fainter band at the monomer position on 7.5% polyacrylamide gel under native and denaturing conditions (Fig. 28). The higher the DHI

concentrations, the less the monomer remained. There was a concurrent deposition of dark substances near the bottom of sample wells. Apparently, DHI concentration-dependently caused BSA to form high molecular weight aggregates that were SDS-stable. The covalent linkage was not reduced by DTT. Particle size measurement on a Zetasizer showed that BSA crosslinked by 2 mM DHI had a molecular weight about 10^8 kDa. After treatment using 0.5 mM DHI, two peaks were detected: one at ~10^6 kDa and the other at

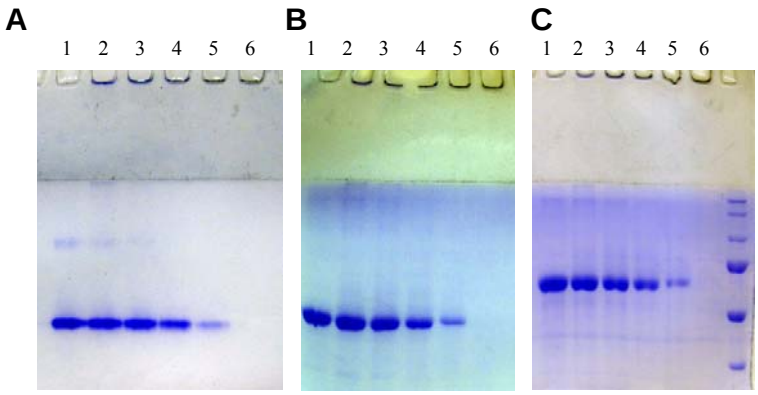

Figure 28. Concentration-dependent reduction of BSA monomer after DHI treatment. A) 7.5% native gel; B) 7.5% SDS-PAGE, nonreducing; C) 7.5% SDS-PAGE reducing. Positions of the molecular size markers (250, 150, 100, 75, 50, and 37 kDa) are indicated. Lanes 1~6: 0, 0.125, 0.25, 0.5, 1.0 and 2.0 mM DHI.

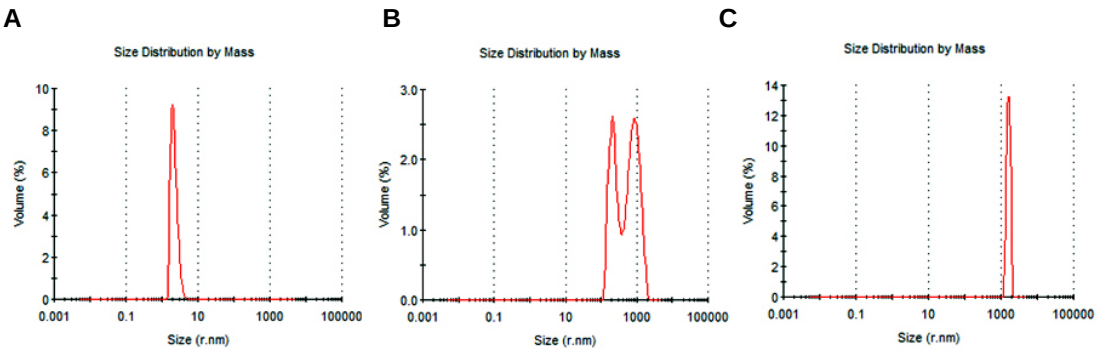

Figure 29. The molecular weight shift of DHI overnight treated BSA measured by Zetasizer. All the samples had been treated with DTT and SDS before measurement A) control BSA without DHI treating B) 0.25 mM DHI treated BSA c) 0.5 mM DHI treated BSA The peak presented the distribution of protein particles in the samples depending on their sizes (radius in nm).

Table 2. The molecular weight of DHI overnight treated BSA measured by Zetasizer

DHI concentration	Molecular weight of peak (kDa)		% Mass	
0 mM	31.0±8.1		99.9	
0.25mM	$1.0\times10^{6}\pm2.97\times10^{5}$	$2.24\times10^{7}\pm8.48\times10^{6}$	40.6	59.4
0.50mM	$1.03\times10^{8}\pm1.17\times10^{7}$		100.0	

The molecular weight of DHI overnight treated BSA increased dramatically. This molecular weight shift can not be disrupted by DTT and SDS. The results of molecular weight were presented as mean ± SD. The % mass results showed ratio of the particles at that size among total detected particles.

~10^{7} kDa. In the negative control, BSA had a molecular mass of ~50 kDa (Fig. 29 and Table 2).

The polymerization of DNA and proteins could explain the antiviral activity of DHI. The aggregation certainly decreases the mobility of virus and abolishes their ability to enter host cells. Beside immobilization, by reacting with cell surface proteins, DHI may block specific virus attachment to cells. If DHI penetrates the virus coat, it is expected to crosslink DNA or RNA molecules to fix their structure through covalent bonds. To bacteria, fungi, and host cells, DHI may crosslink cell surface receptors and lead to abnormal cell signaling. Inside the cells, DHI may aggregate cytosolic proteins and trigger apoptosis. DHI modification of actin, the most abundant protein in cell, could cause it to further polymerize, change cytoskeleton, and rupture the cells.

10. Cytoskeletal structural changes after DHI-treatment – Phalloidin, a toxic protein from the death cap mushroom, specifically bind to filamentous actin (F-actin). Using labeled phalloidin, we detected some small patches on the green background: F-actin was quite evenly distributed in the control *Sf*9 cells (Fig. 30). DHI-treated cells showed condensed green signal around the nuclear region or as spike-like bundles, indicative of abnormal remolding of actin polymer. Some actin bundles of were present at regions without cell

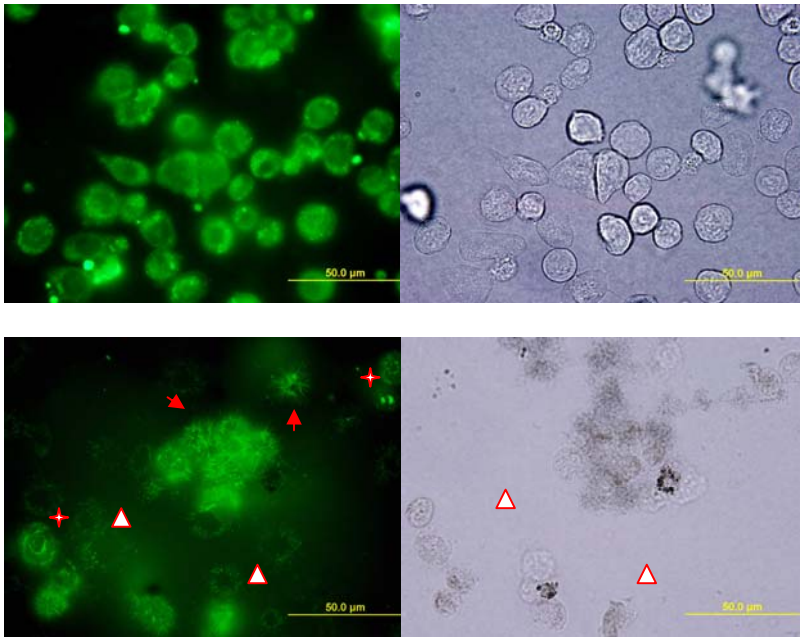

Figure 30. Untreated and DHI-treated *Sf*9 cells stained with Oregon Green 448-conjugated phalloidin. Top: control cells under fluorescence (*left*) and bright field (*right*). Bottom: DHI-treated. Condensed green signals were observed around nuclear region (Star), as spike-like bundles (arrow), and in areas without cellular structure (open triangle).

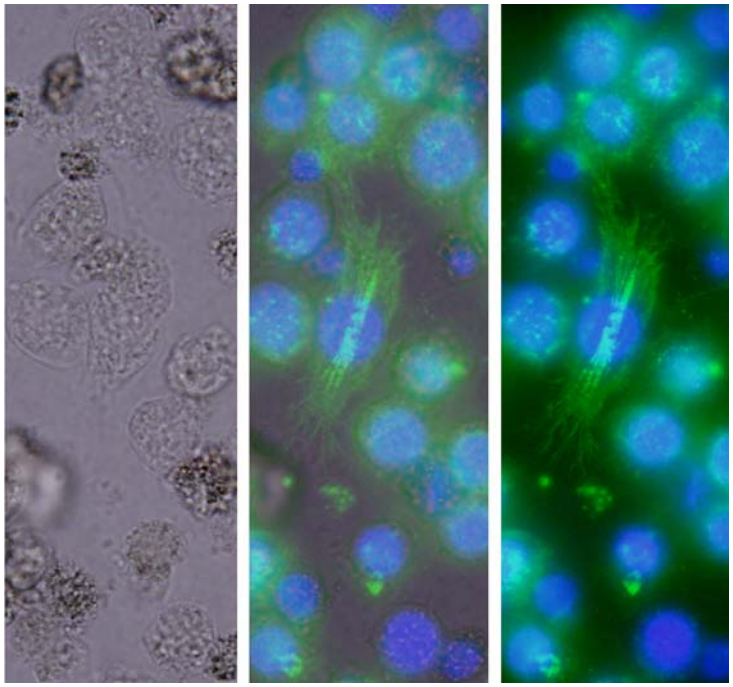

Figure 31. Bright field (left), fluorescent (right), and merged (middle) images of DHI-treated *Sf*9 cells stained with Oregon Green 448-conjugated phalloidin and DAPI.

structure, as revealed by comparison of fluorescence and bright field images. These bundles were probably attached to the glass surface. In a different set of images, some F-actin polymers may have penetrated the cell membrane (Fig. 31). To better demonstrate the positions of F-actin in relation to cytoplasmic membrane, we used SYTO 9 in conjunction with Alexa Fluor 568 (red) conjugated phalloidin and DAPI (a blue nucleus dye). SYTO 9, a membrane-permeable dye preferably binding to RNA, emits green light and shows cytoplasmic staining. As shown in Fig. 32, red signals of actin spikes clearly went beyond the cytoplasmic region. Consistent with the earlier observation (Fig. 30), signals of F-actin were also detected in regions where no cellular structure was present. Taken together, these data suggest that abnormal remolding of actin broke plasma membrane and facilitated the release of cell contents. We do not know the driving force of the cell polarization and how DHI triggers this process of polarization and rupture of cell membrane. One possibility is that DHI and its oxidation products crosslink and aggregate motor proteins and microtubule.

Further examination was done about whether or not DHI-induced abnormal actin remodeling occurred before cell death by combining phalloidin staining with DAPI and PI. DAPI is membrane permeable, whereas membrane-impermeable PI only stains the nucleus of cells with broken plasma membrane (*i.e.* dying or dead cells). Under the test conditions, most living cells were healthy and had green F-actin signals quite evenly distributed in cytoplasm (Fig. 33). Some living cells showed condensed F-actin signals around the nuclear region, while others contained actin bundles. Since these cells were stained by DAPI only, abnormal actin remodeling happened before cell death and may contribute to cell death. In other words, DHI and its oxidization products seemed to be

able to penetrate the membrane of living cells, react with cellular proteins and/or nucleic acids, and trigger cell polarization, rupture, and death.

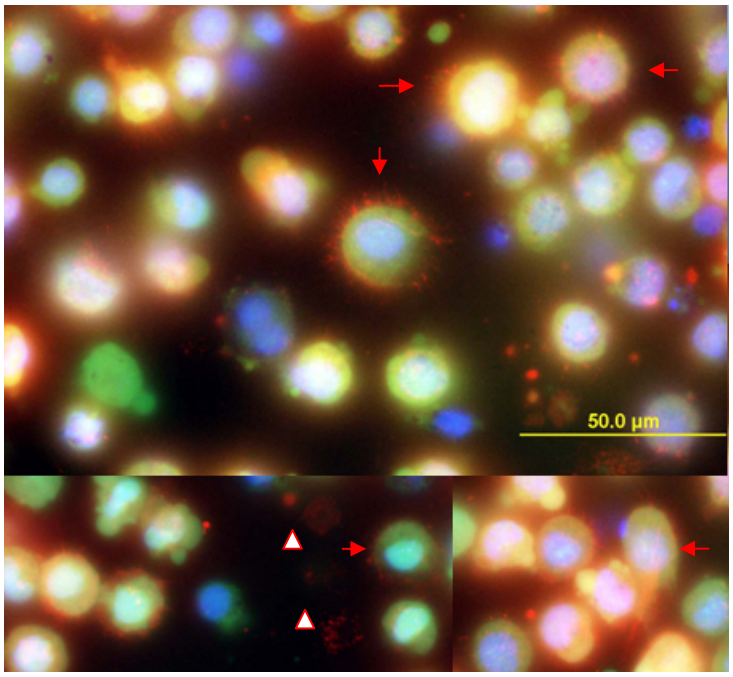

Figure 32. DHI-treated *Sf*9 cells stained with Alexa Flouor 568-conjugated phalloidin, SYTO9 and DAPI. Actin bundles (red, *arrow*) extended beyond cytoplasm region (green). Actin bundles can be observed in areas lacking cellular structure (triangle).

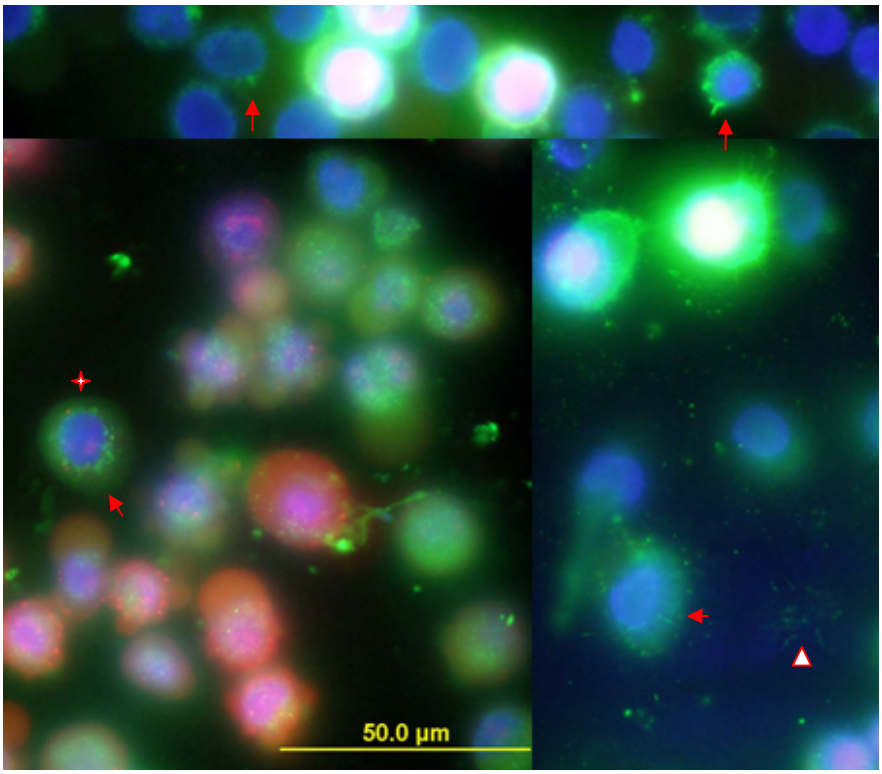

Figure 33. DHI-treated *Sf*9 cells stained with Oregon Green 448-conjugated phalloidin (green), PI (red) and DAPI (blue). Living cells showed green and no red signal (*i.e.* PI negative). Dead cells showed red (*i.e.* PI positive). All cells nuclear region stained by DAPI showed blue. Strong green, blue and red signals combine to show white. Condensed green signal around nuclear region (star) and spike-like bundle (arrow). Actin bundles signal can be observed in areas lacking cellular structure (triangle)

Objective 2: Expression and functional characterization of *M. sexta* serpin-10

1. Phylogenetic analysis of *M. sexta* serpin-10 and its homologs -- By comparing with the silkworm serpin genes, we found *M. sexta* serpin-10 is orthologous to *B. mori* serpin-13 (Fig. 34), *Anopheles gambiae* and *Aedes aegypti* serpin-6, *Apis mellifera* serpin-4, *Tribolium castaneum* serpin-27, and *Drosophila melanogaster* serpin28D [Zou et al., 2009]. Genetic analysis of *Drosophila* serpin28D showed that it regulated hemolymph PO activity and adult pigmentation [Scherfer et al., 2008].

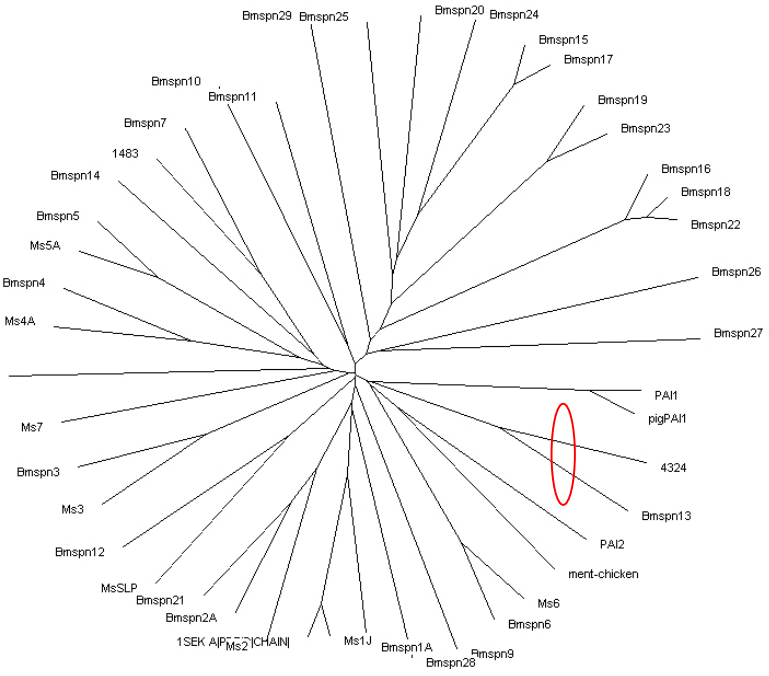

Figure 34. Phylogenetic relationships among the serpins from *B. mori*, *M. sexta*, and other animals. To confirm classification as serpins, the protein sequences were scanned for domain features using CDART [Geer et al., 2002], PROSITE, and SMART [Schultz et al., 1998, Ponting et al., 1999; Letunic et al., 2009]. Signal peptides were predicted by SignalP3.0. Complete serpin domains were aligned using ClustalX 1.83[Thompson et al., 1994; Thompson et al., 1997]. Phylograms were displayed by neighbor-joining analysis through Treeview [Page, 2002]. A Blosum 30 matrix, with a gap penalty of 10 and an extension gap penalty of 0.05 were selected for the multiple sequence alignment.

2. Transcriptional regulation of *M. sexta* serpin-10 – We examined the gene expression in different larval tissues and found the mRNA was present most abundantly in nerve tissue

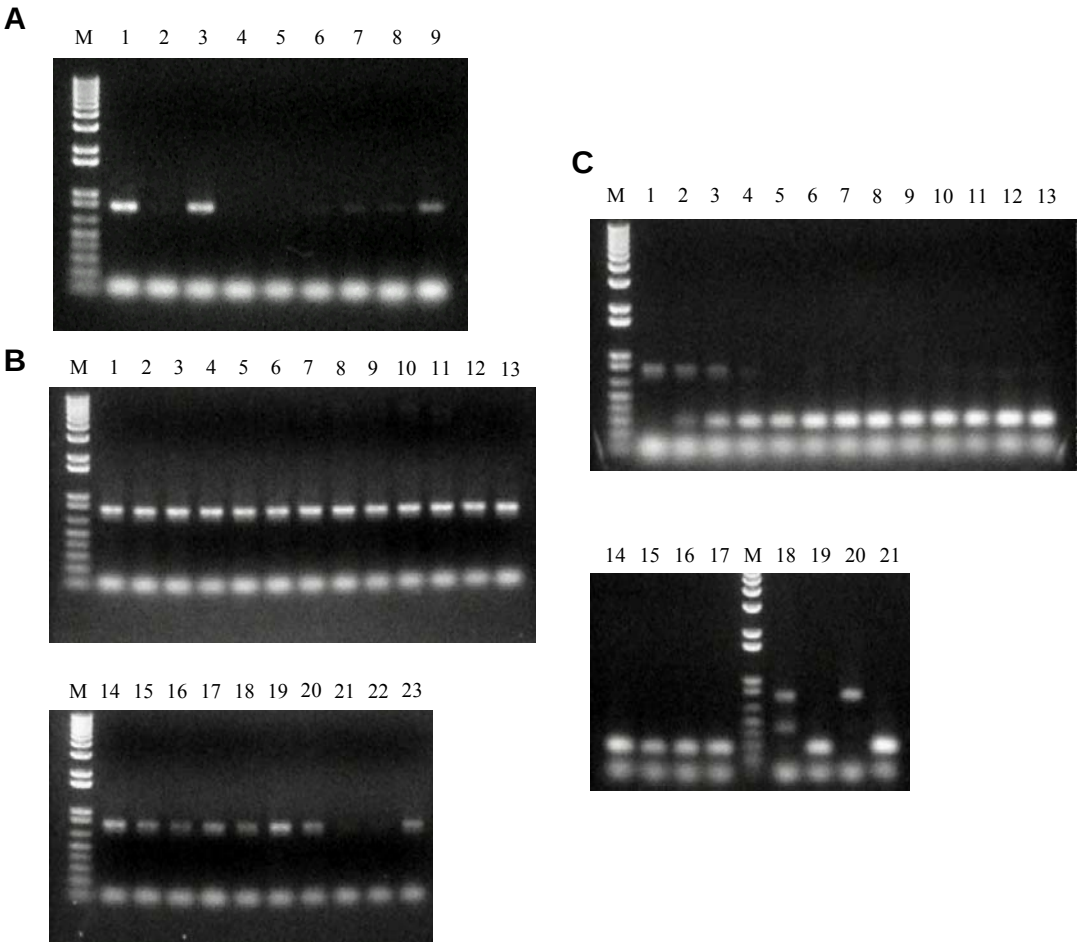

Figure 35. RT-PCR analysis of MsSerpin10 mRNA levels in different disuses (**A**), life stage (**B**), and immune status (**C**). In **A**, 1: nerve tissue, 2: salivary gland, 3: trachea, 4: Malpighian tubule, 5: Mid-gut, 6: integument, 7: muscle, 8: hemocytes, 9: Fat body. The higher bands are the specific products of MsSerpin10. 0.1 μL cDNA, 35 cycles. In **B**, lanes 1-6: 4th instar day 0, 1, 2, 3, 4, 5; lanes 7-13: 5th instar, day 0, 1, 2, 3, 4, 5, 6; lanes 14-19: wandering stage, day 1, 2, 3, 4, 5, 6; lanes 20-23: early pupal, middle pupal, late pupal, and adult stages. 0.1 μL cDNA, 35 cycles. In **C**, lanes 1-17: 0, 1.5, 3, 4.5, 6, 7.5, 9, 10.5, 12, 13.5, 15, 16.5, 18, 19.5, 21, 22.5, 24 h after the immune challenge; lanes 18-21. 24 h, naïve hemocytes, induced hemocytes, naïve fat body, and induced fat body. 0.2 μL cDNA, 50 cycles. Top band, serpin10; bottom band, rpS3 (an internal reference), middle band (in panel **C**), hemolin (positive control).

and trachea, followed by fat body (Fig. 35A). There was no substantial change in levels of MsSerpin10 transcripts in fat body during 4th instar and 5th instar. At wandering stage, the mRNA decreased after day 1 (Fig. 35B). A significant decrease in serpin-10 mRNA

occurred at middle and late stage of pupa, followed by an increase in transcription in the adult. To test its possible role in immunity, we used the specific primers and amplified the serpin10 cDNA fragment from fat body and hemocytes naïve larvae. However, we did not detect the serpin mRNA in the two tissues from insects injected with bacteria (Fig. 35C). The suppression of gene expression was confirmed by detailed analysis of fat body samples taken at different times after the immune challenge. While serpin10 transcript level decreased and reached its lowest at 4.5 h, there was an increase of hemolin mRNA from its immune inducible gene.

3. Recombinant expression of *M. sexta* serpin-10 – To study its function, we amplified a cDNA fragment of *M. sexta* serpin-10 and inserted the *Eco*RI-*Xho*I fragment into the same sites in $pMFH_6$. DNA sequence analysis showed that the insert was identical to the template. The serpin domain was correctly fused with the honeybee mellitin signal peptide and carboxyl-terminal affinity tag encoded by the vector [Lu and Jiang, 2008].

Using *Ms*Spn10/$pMFH_6$, we generated a recombinant baculovirus that infected *Sf*9 cells and expressed the recombinant protein in a soluble form. We applied the sample onto a DS-Sepharose column to remove medium and DNA and eluted proteins with a high salt buffer. The binding of *Ms*Spn10 to Ni-NTA agarose was no longer interfered by medium components or nucleic acids. The protein strongly associated with beads in the presence of 30 mM imidazole while other proteins did not bind. Finally the serpin was separated from other contaminants by S-100 gel filtration chromatography. As demonstrated by 10% SDS-PAGE and Coomassie blue staining, the protein was close to homogeneity, which migrated as a broad band at ~52 kDa (Fig. 36).

4. Specificity of serpin-10 antiserum -- The purified recombinant *M. sexta* serpin-10 (0.5

mg) was used as an antigen for the preparation of a rabbit polyclonal antiserum. Using a panel of six *M. sexta* serpins (serpin-1, 3, 5, 6, 8, 10), we examined the specificity of serum from the final boost. The antiserum reacted strongly with serpin-10 and showed some cross-reactivity with serpin-3 (Fig. 37).

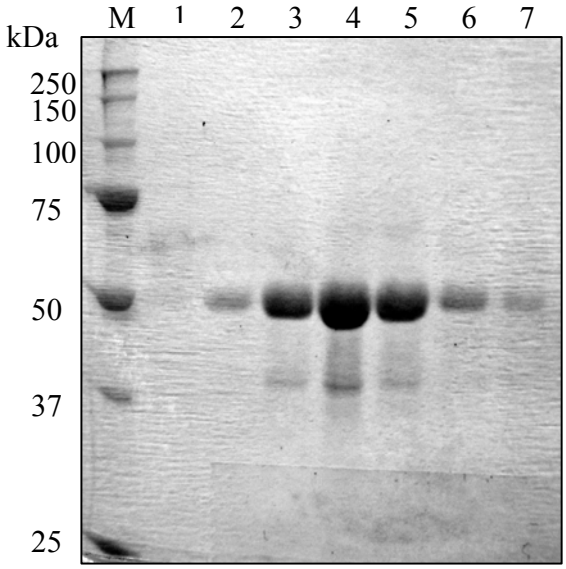

Figure 36. 10% SDS-PAGE analysis of recombinant serpin-10 fractions from gel filtration chromatography on Sephacryl S100 column. The protein bands shows at the anticipated size (~50 kDa). M: protein size marker; lanes 2-8: 12 µL/lane of sample from the factions.

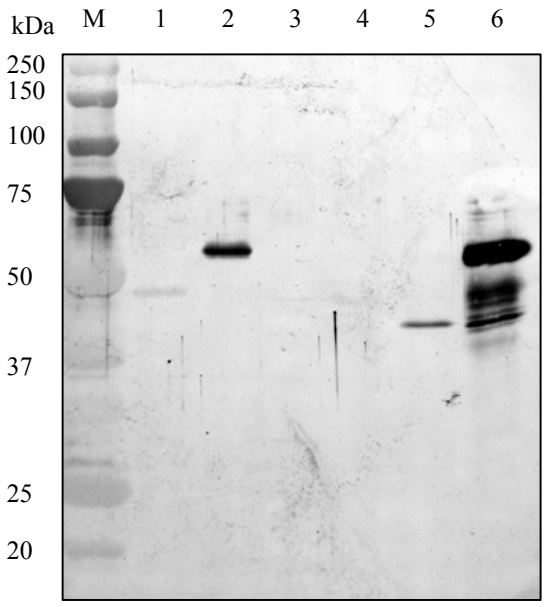

Figure 37. Western blot detection of possible cross-reactivity of serpin10 antibodies to the other recombinant serpins of *M. sexta*. Lanes 1~6: *M. sexta* serpin-1, -3, -5, -6, -8, and -10 at 5 ng/lane, respectively. 1st antibody: 1:2000 diluted serum against serpin-10.

5. Isolation of serpin-10-containing immune complex – On the Coomassie blue stained gel, we detected 100, 75, 52, 35, 30 kDa proteins eluted from the serpin-10 antibody column (Fig. 38). Much less proteins were found in samples from the control column. The 52 kDa major band and its cleaved products (~47 kDa) were strongly recognized by the serpin-10 antibodies. Other immunoreactive proteins included 95, 86, 78 kDa bands that are not detected in the control sample. When we compared the samples with control and induced plasma, there was a clear enrichment of 78, 52, and 47 kDa bands and removal of storage proteins that distorted the banding pattern of plasma samples (Fig. 39). The 78 kDa band may represent the covalent complex of serpin-10 and an unknown HP catalytic domain.

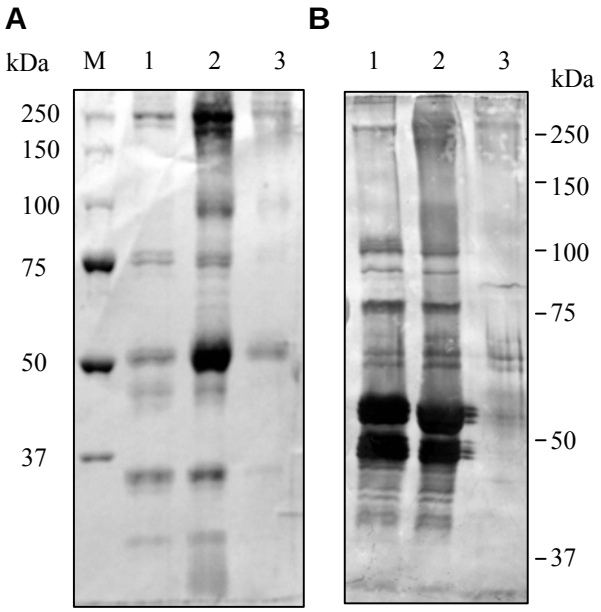

Figure 38. Coomassie blue (A) and Western blot (B) detection of plasma proteins eluted from the serpin-10 antibody column. (A) 7.5% SDS-PAGE gel stained with Coomassie blue. (B) Western blot using *M. sexta* serpin-10 antibodies. 10 µL/lane. M, protein size markers, lane 1, induced plasma with serpin-10 antibody column; lane 2, control plasma (from naïve larvae) with serpin-10 antibody column; lane 3, control plasma with pre-immune antibody column.

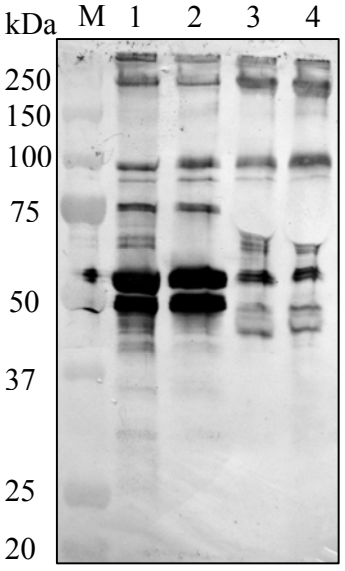

Figure 39. Western blot comparison of affinity-purified proteins and plasma samples. The column-bound proteins and plasma were loaded at 10 and 1 µL/lane, respectively. The 1st antibody: 1:2000 diluted *M. sexta* serpin-10 antiserum. M, protein size markers; Lane 1, bound proteins from control plasma; Lane 2, bound proteins from induced plasma; Lane 3, control plasma; Lane 4, induced plasma.

In order to characterize the 78 kDa band, the activated control hemolymph was fractionated with ammonia sulfate, hydroxyapatite chromatography, and ion exchange chromatography on a dextran sulfate column. After the antibody column, two major bands were detected on the Coomassie blue stained gel: one at 70 kDa and the other at 52 kDa (Fig. 40). While the 52 kDa protein was confirmed to be serpin-10, the 77 kDa signal was very weak on the immunoblot (data not shown).

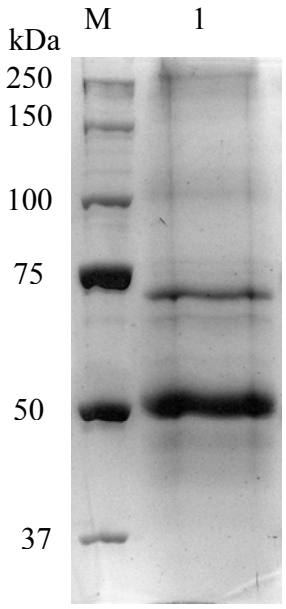

Figure 40. 7.5% SDS-PAGE analysis of the antibody-recognized protein complex from the ammonium sulfate precipitation, ion exchange, and affinity chromatography fractionated plasma sample. The activated control hemolymph, after purified by ammonia sulfate precipitation, hydroxyapatite chromatography, dextran sulfate chromatography and affinity chromatography, showed less background on 7.5% SDS-page Coomassie blue stained gel. There is one clear band at about 50 kDa and one at about 70 kDa. M, protein size markers; lane 1, bound proteins from pre-purified plasma.

6. Identification of components in the serpin10-containing immune complex by HPLC-MS-MS – Mass spectrometric analysis of the protein samples directly eluted from the affinity chromatography showed MsSerpin10 signal at around 50 kDa and 70~80 kDa, along with many other proteins (Fig. 41). The original size of MsSerpin10 is about 50

kDa; the signal at 70~80 kDa may represent a complex formed between serpin10 and its unknown target serine protease. We detected MsHP1 signal at about 50 kDa. In comparison, the sample after AS fractionation, ion exchange and immunoaffinity chromatography showed a lot fewer proteins were pulled down with MsSerpin10 (Fig. 40 and Fig. 42). Apparently, "sticky" proteins once associated with the complex were removed in the purification steps. Much lower signals of storage proteins were detected. MsSerpin10 signals were again found at about 50 and 70~80 kDa. HP1 signal was detected at around 50 kDa and, hence, MsHP1 is likely a non-covalently associated component of the immune complex containing MsSerpin10. In contrast, immunity-related protein SPH1 was pulled down by direct affinity chromatography but did not show up in the pre-purified sample.

Since MsSerpin10 signal was detected at the size of a serpin-protease complex, we assumed that the complex had been pulled down by the serpin antibodies. Unfortunately, we failed to identify such a target protease (Fig. 41). It can be due to the lack of sequence information of this protease in our *M. sexta* hemolymph protein database. The attempt to reduce other proteins around 70~80 kDa was successful through the purification steps: only one band was detected at around 70 kDa (Fig. 40), which was determined to be PPO. However, the level of presumed serpin-protease complex did not largely increase in relative to contaminating proteins. Consequently, I did not obtain suffcient amount of complex for *de novo* protein sequencing or identification (Fig. 42). The *M. sexta* genome sequence is anticipated to facilitate the elucidation of Msserpin10 target enzyme.

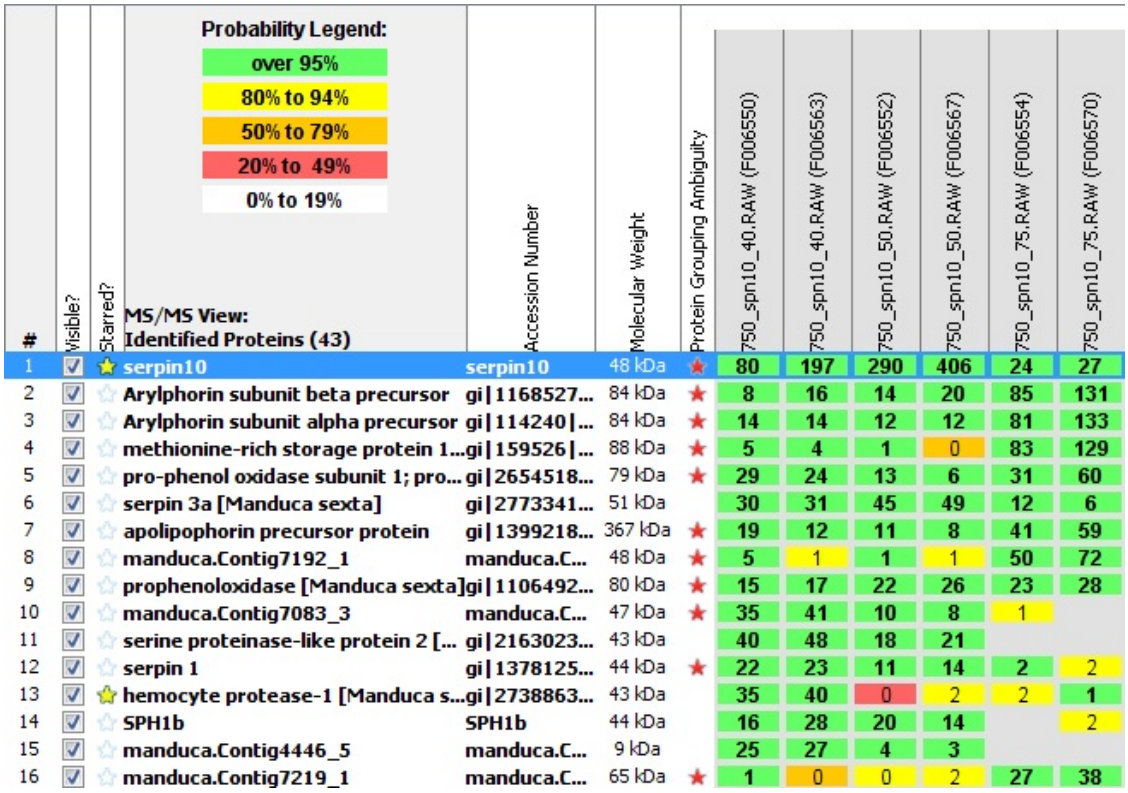

Probability Legend:
over 95%
80% to 94%
50% to 79%
20% to 49%
0% to 19%

#	Visible?	Starred?	MS/MS View: Identified Proteins (43)	Accession Number	Molecular Weight	Protein Grouping Ambiguity	750_spn10_40.RAW (F006550)	750_spn10_40.RAW (F006563)	750_spn10_50.RAW (F006552)	750_spn10_50.RAW (F006567)	750_spn10_75.RAW (F006554)	750_spn10_75.RAW (F006570)
1	☑	★	serpin10	serpin10	48 kDa	★	80	197	290	406	24	27
2	☑	☆	Arylphorin subunit beta precursor	gi|1168527...	84 kDa	★	8	16	14	20	85	131
3	☑	☆	Arylphorin subunit alpha precursor	gi|114240|...	84 kDa	★	14	14	12	12	81	133
4	☑	☆	methionine-rich storage protein 1...	gi|159526|...	88 kDa	★	5	4	1	0	83	129
5	☑	☆	pro-phenol oxidase subunit 1; pro...	gi|2654518...	79 kDa	★	29	24	13	6	31	60
6	☑	☆	serpin 3a [Manduca sexta]	gi|2773341...	51 kDa		30	31	45	49	12	6
7	☑	☆	apolipophorin precursor protein	gi|1399218...	367 kDa	★	19	12	11	8	41	59
8	☑	☆	manduca.Contig7192_1	manduca.C...	48 kDa	★	5	1	1	1	50	72
9	☑	☆	prophenoloxidase [Manduca sexta]	gi|1106492...	80 kDa	★	15	17	22	26	23	28
10	☑	☆	manduca.Contig7083_3	manduca.C...	47 kDa	★	35	41	10	8	1	
11	☑	☆	serine proteinase-like protein 2 [...	gi|2163023...	43 kDa		40	48	18	21		
12	☑	☆	serpin 1	gi|1378125...	44 kDa	★	22	23	11	14	2	2
13	☑	★	hemocyte protease-1 [Manduca s...	gi|2738863...	43 kDa		35	40	0	2	2	1
14	☑	☆	SPH1b	SPH1b	44 kDa		16	28	20	14		2
15	☑	☆	manduca.Contig4446_5	manduca.C...	9 kDa		25	27	4	3		
16	☑	☆	manduca.Contig7219_1	manduca.C...	65 kDa	★	1	0	0	2	27	38

Figure 41. NanoLC-MS-MS identification of proteins directly isolated from plasma by the serpin antibody affinity column.

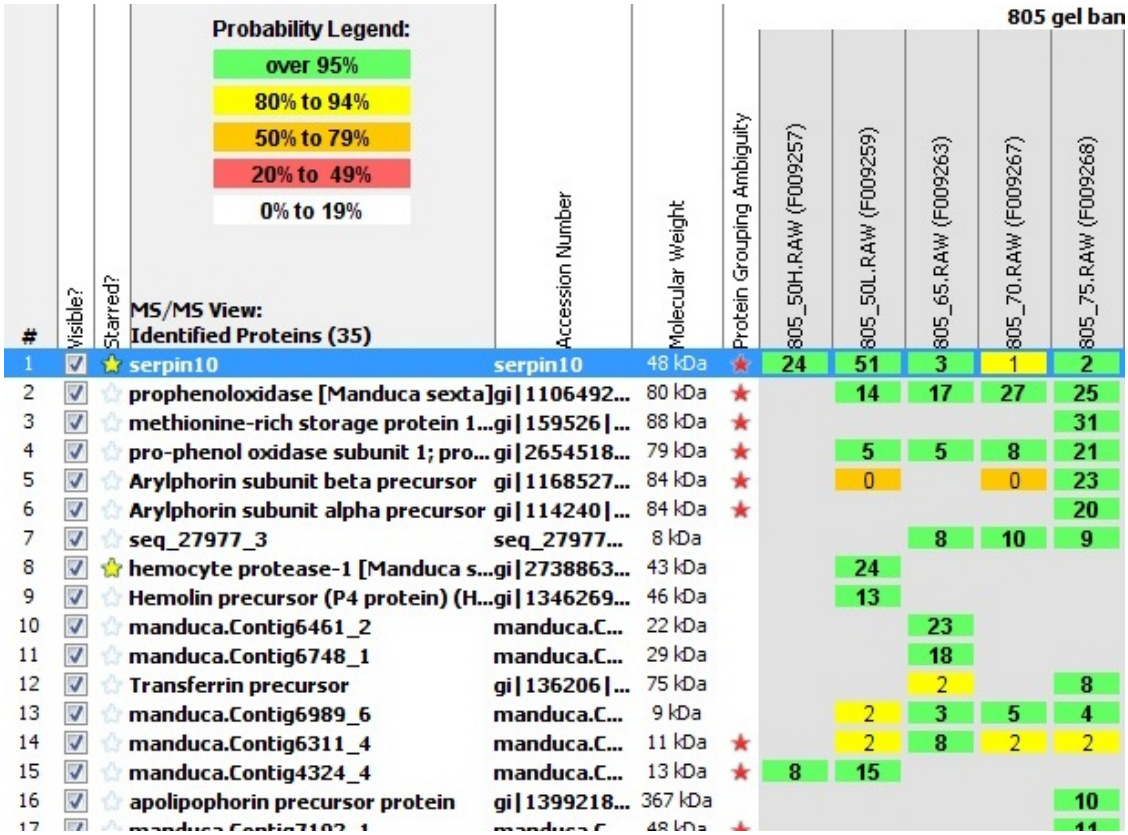

Probability Legend:
over 95%
80% to 94%
50% to 79%
20% to 49%
0% to 19%

805 gel ban

#	Visible?	Starred?	MS/MS View: Identified Proteins (35)	Accession Number	Molecular Weight	Protein Grouping Ambiguity	805_50H.RAW (F009257)	805_50L.RAW (F009259)	805_65.RAW (F009263)	805_70.RAW (F009267)	805_75.RAW (F009268)
1	☑	★	serpin10	serpin10	48 kDa	★	24	51	3	1	2
2	☑	☆	prophenoloxidase [Manduca sexta]	gi|1106492...	80 kDa	★		14	17	27	25
3	☑	☆	methionine-rich storage protein 1...	gi|159526|...	88 kDa	★					31
4	☑	☆	pro-phenol oxidase subunit 1; pro...	gi|2654518...	79 kDa	★		5	5	8	21
5	☑	☆	Arylphorin subunit beta precursor	gi|1168527...	84 kDa	★		0		0	23
6	☑	☆	Arylphorin subunit alpha precursor	gi|114240|...	84 kDa	★					20
7	☑	☆	seq_27977_3	seq_27977...	8 kDa				8	10	9
8	☑	☆	hemocyte protease-1 [Manduca s...	gi|2738863...	43 kDa			24			
9	☑	☆	Hemolin precursor (P4 protein) (H...	gi|1346269...	46 kDa			13			
10	☑	☆	manduca.Contig6461_2	manduca.C...	22 kDa				23		
11	☑	☆	manduca.Contig6748_1	manduca.C...	29 kDa				18		
12	☑	☆	Transferrin precursor	gi|136206|...	75 kDa				2		8
13	☑	☆	manduca.Contig6989_6	manduca.C...	9 kDa			2	3	5	4
14	☑	☆	manduca.Contig6311_4	manduca.C...	11 kDa	★		2	8	2	2
15	☑	☆	manduca.Contig4324_4	manduca.C...	13 kDa	★	8	15			
16	☑	☆	apolipophorin precursor protein	gi|1399218...	367 kDa						10

Figure 42. NanoLC-MS-MS identification of proteins isolated by ammonium sulfate fractionation, ion exchange and MsSerpin10 antibody affinity chromatography.

3. Discussion

a. DHI in other animals

Melanization, occurring in a wide variety of organisms, is related to many physiological processes and pathological phenomena. Extensive physical, chemical and toxicological research has been performed on melanization in mammals. Melanin exists in different cell types including melanoma cells, retinal cells, and macrophages. It is related to thermoregulation, photo-protection, and melanoma. The pigmentation in melanoma cells can protect them from UV at different wavelengths [Hill and Hill, 2000]. In amphibian Kupffer cell of *Rana esculenta*, tyrosinase catalyzes melanogenesis, which is not affected by catalase or H_2O_2 [Gallone et al., 2007]. In mouse macrophages, a melanin precursor DHIAC can increase the production of nitric oxide (NO) that is normally produced by LPS-induced NO synthase [D'Acquisto et al., 1995]. Melanin can be a regulator for the calcium homeostasis of endolymph [Gill and Salt, 1997]. Although the precursor is cytotoxic, melanin is believed to be able to protect the cells by neutralizing reactive oxygen species [Wood et al., 1999]. At low concentrations, DHI exhibits protective effect to retinal cells both *in vivo* and *in vitro*, but at high concentrations it shows high cytotoxicity *in vitro* [Heiduschka et al., 2007]. Function of melanin is still a controversial topic. From current research we can see its roles in both toxicity and protection. As an important process in different organisms, melanization is under strict regulation to ensure its proper function.

b. Two types of melanin

Melanin can be divided into two main types: eumelanin (dark brown to black) and phaeomelanin (yellow to reddish brown) [Tody et al., 1991, Hunt et al., 1995]. In

melanosomes of melanocytes in human skin, the ratio of these two types is related to pH, which may be regulated by P-protein [Ancans et al., 2001]. Dopaquinone (DQ), the oxidation product of L-tyrosine or L-DOPA, is a common precursor of both eumelanin and phaeomelanin [Ito and Wakamatsu, 2008]. The intramolecular linking of amino group of DQ forms cyclodopa, which leads to DHI and eumelanin formation [Land and Riley, 2000]. Addition of cysteine to DQ will form cysteinyldopa (CD) isomers, which leads to the phaeomelanin formation [Napolitano et al., 1999]. In insects, there is no report about the formation of phaeomelanin. But insects have tyrosinase-type POs which, along with other enzymes, can generate eumelanin through tyrosine-DQ-dopachrome-DHI process. Dopa can be converted into dopamine and oxidized by POs into dopamine quinone which cyclizes to form DHI. PO is the key enzyme that can catalyze oxidization steps for eumelanogenesis in insects [Sugumaran, 2002; Nappi and Christensen, 2005].

c. Hemocyte responses

Little is known of the molecular mechanisms that activate hemocytes and initiate melanogenesis in response to infection. Typically, parasite-induced melanization is cell-mediated, site-specific, and does not provoke undesirable systemic activation in the host's open circulatory system. In insects like mosquitoes that possess a limited number of circulating hemocytes, melanization of parasites appears to be primarily a humoral response. This was found in studies involving melanization of *Plasmodium* [Collins et al., 1991; Lanz-Mendoza et al., 2002] and filarial worms [Beerntsen et al., 2000]. On the other hand, mosquito hemocytes are employed in the melanization and phagocytosis of bacteria [Hillyer et al., 2003a, 2003b, and 2005].

d. Antiviral immunity

Insects can be infected by pathogenic viruses in a natural environment and the resistance of some insects to viruses has been documented [Cory and Myers, 2003, Kirkpatrick et al., 1998]. Protection of host against virus was reported, and the hemocyte aggregation is essential for avoiding virus spreading [Washburn et al., 1996, Clarke and Clem, 2002]. The antiviral activity of insect hemolymph has been reported [Popham et al., 2004]. But there are still controversies whether PO is truly involved in antiviral response. One recent paper [Saejeng et al., 2010] reported hemolymph PO activity in asymptomatic resistant *Plodia interpuncetella*, similar to uninfected control larvae hemolymph, did not change after *P. interpunctella* granulosis virus (PiGV) infection. On the contrary, they found PO activity clearly increased after PiGV infection in symptomatic susceptible larvae. They concluded that PO may not be immunocompetent against viral infection in their system. In my opinion, the method they used for measuring specific PO activity may be erroneous. Resistance to viral infection is caused by a number of reasons and is not equivalent to PO activity. Besides immune responses, other important mechanisms such as blocking virus-host cell interaction, disrupting fusion of virus with cells, or hiding/losing specific interaction site could all lead to resistance [De Clercq et al., 2002, Hyman and Abedon, 2010]. For instance, in innate immunity of mammals, some Toll-like receptors, which are sensors of virus recognition, locate in intracellular cytoplasmic compartment [Ahmad et al., 2002, Kawei and Akira, 2006]. If the virus can not enter the cell, they cannot cause any infection and will not be recognized by the Toll-like receptors to trigger immune responses. Another report showed that, in *Lymantria dispar* larvae, multiple nucleocapsid nucleopolyhedrovirus

(LdMNPV) infection generated more potential PO activity and tissue melanization. The virus infection was reduced [McNeil et al., 2010].

The polymerization of biological macromolecules, such as DNA and proteins, and partial inactivation of *Sg*AChE1 by DHI explain its antiviral activity. The aggregation may decrease the mobility of virus and abolish their ability to access host cells. Besides immobilization, DHI may also block interaction with specific surface proteins by reacting with viral coat proteins critical for attaching to cell. If DHI penetrates the protein coat of a virus, it may react with nucleic acids and cause abnormal covalent bond formation which changes their topology.

The antiviral activity of DHI was first revealed by comparing *Sg*AChE1 activity levels in cultures infected with the untreated and treated baculovirus. The evidence was indirect and the enzyme activity may poorly correlate with viral titers – unknown ratio of infection, expression level fluctuation, and activity assay may all lead to accumulation of system errors. On the other hand, the λ-phage plaque assay directly quantifies the viability loss caused by DHI treatment.

e. Spectrum of the antibiotic activity

We found that the roles of melanization include anti-bacterial, anti-fungal, anti-viral, and anti-parasitic responses. This reaction has a broad-spectrum for all possible agents that can invade insects. This kind of universal killing power seems to stem from its basic mechanism of toxicity. Melanization is a complex process involving an enzyme-regulator system. The co-evolution of anti-melanization virus from parasitoid wasps indicates it may be one of the key factors deciding their survival during natural selection. So it is logical to believe melanization is an essential component of the insect innate

immune system. It seems unreasonable if insects need to apply so much energy into synthesizing the components for activating and regulating an unnecessary process.

f. Cytotoxicity

In many cases, melanization response works as a two blade sword. As an active compound, DHI not only attacks invading microbes and parasites but also shows high toxicity to host cells. The death of infected cells can be regarded as a sacrifice to prevent further infection by the microorganism to adjacent healthy tissues. The balance between resistance and tolerance to infection is delicate so that it can be broken just by a single mutation [Ayres et al., 2008]. The regulation of this process, therefore, is strict and involves different participants [Lu and Jiang, 2007, Clark et al., 2010]. Overreaction of the immune response is extremely harmful. The larval death of a serpin mutant clearly demonstrated the importance of PPO activation cascade regulation [Leclerc et al., 2006].

We can partly describe the process of cell content release after DHI treatment. In cells undergoing early apoptosis, some organelles and nucleus start to polarize but plasma membrane remains intact and cells are alive in the beginning. With the plasma membrane breaking, cell contents are released. In the broken cells, both Annexin V and PI can cross the plasma membrane and stain the cell. Although these cells can be stained as Annexin V positive and PI negative in the beginning, this process does not perfectly match the classic description of apoptosis. The releasing process is similar to the formation of blebs (*i.e.* apoptotic bodies) in apoptosis and most released cell contents can be stained by Annexin V, which suggests they are enveloped in the plasma membrane. Compared with apoptotic bodies, these structures are much bigger, some of them even containing a whole nucleus along with other organelles. The DNA fragmentations from DHI treated cells

samples indicate the activity of execution caspases. So the DHI-treated insect cells showed some features of apoptosis: Annexin V positive, PI staining negative, and DNA fragmentation. Just the release of structures including whole nucleus makes it different from apoptosis. We may name it “macrovomitus” to better describe the cellular process.

To cells including bacteria, fungi and host cells, DHI may crosslink cell surface receptors from outside and cause anormaly in cell signaling. For example, the dimerization of initiator (apical) caspases is a crucial step of their activation [Riedl et al., 2007]. If DHI does facilitate their dimerization, this can directly activate the effector (executioner) caspases and start apoptosis. Indeed, we detected apoptosis signal in DHI-treated insect cells and DNA fragmentation.

Inside cells, DHI may cause cytosolic proteins to polymerize via crosslinking. For example, abnormal polymerization of actin, the most abundant protein in cells, may lead to changes in cytoskeleton. Since we have observed penetration of actin bundles out of plasma membrane, it is likely the plasma membrane of DHI-treated cells was broken. Evans Blue and PI-staining also indicated the damage of plasma membrane. Another type of cytoskeleton, microtubules are very dynamic on assembly and disassembly in a GTP-dependent way [Howard and Hyman, 2003]. It is perhaps reasonable to assume that microtubules may be involved in providing driving forces to the polarization of cell contents, and the actin abnormal remoldeling caused plasma membrane to break and that facilitated the release of cell contents.

The abnormally formed actin bundles inside of the cells can be dangerous. Like spikes, they may poke into different organelles and cause mechanical damage to cells. This kind of damage may cause leakage of cytochrome C from mitochondria or dATP

from nucleus. Both of them are essential cofactors for forming apoptosome, which can initiate programmed cell death [Riedl et al., 2007]. But if the actin spikes break plasma membrane, it is more like physical damage that causes cell necrosis. It is hard to determine the DHI-induced cell death as apoptosis or necrosis. This is not typical and can be a combination of both.

g. Action mechanisms of DHI

Polymerization of DHI oxidized products can be one reasonable mechanism for its toxicity. The antiviral activity indicates its toxicity comes from effect on protein or nucleic acid. That is why we design the experiment of DNA and protein treatment. The process of DHI-induced molecular crosslinking depends on transient dipole strength [Riesz et al., 2007]. The formation of rigid polymer during DHI oxidization has been illustrated, and a macrocircular structure motif is predicted to be the backbone module of eumelanin [Arzillo et al., 2010]. We believe these polymers works as strong hinges, linking different biological macromolecules to form polymers. We do not have any evidence to describe what had happened to those polymerized DNA or protein molecules. For instance, is there conformational change? We can only say that the loss of catalytic activity of *Sg*AChE1 after treated by DHI. This kind of activity loss may be related to the limited access of enzyme to incoming substrate or releasing products. We did not detect any degradation after the plasmid DNA, linear or circular, were treated by DHI.

CHAPTER V

CONCLUSION

1. Antibiotic activities of PO-generated reactive compounds

In this work, we studied antibiotic effect of the reactive intermediates produced in PO-catalyzed reactions. After being treated with *M. sexta* PO and dopamine, *E. coli* and *B. subtilis* ceased to grow whereas the growth of *P. pastoris* was slightly affected. Microscopic analysis showed melanin deposition on cell surface, aggregation of bacteria, and loss of cell mobility. Viability tests revealed a major decrease in the bacterial colony counts and, since the decrease remained significant after dispersion of the cell clumps, the reactive compounds had aggregated and killed *E. coli* and *B. subtilis* cells. Under the experimental conditions, 16-40% of the Gram-negative bacteria (*E. coli*, *K. pneumoniae*, *P. aeruginosa* and *S. typhimurium*) and 1-48% of the Gram-positive bacteria (*B. cereus*, *B. subtilis*, *M. luteus* and *S. aureus*) survived after the treatment. DHI and its spontaneous oxidation products were also active against viruses and parasitic wasp eggs. Over 97% of the baculoviruses were killed after 3 h treatment with 1.25 mM DHI and the LC_{50} for lambda bacteriophage was 5.61 ± 2.21 μM, suggesting proPO activation is a component of the antiviral response in insects.

2. Cytotoxicity of DHI to insect cells

The toxicity of DHI and related compounds is not limited to invading organisms

(*e.g*., bacteria, fungi, viruses, and parasitoids): after being treated with 1 mM DHI, 97.2% of the *S. frugiperda Sf*9 cells were dead and LC_{50} was 20.3 ± 1.2 μM. This result suggests that proPO activation, if not properly controlled, could damage host tissues and cells as well. Regulatory mechanisms, therefore, have to be in place to ensure this broad-spectrum antibiotic activity is a local, transient response against none-self. A possible mechanism of DHI toxicity is the cross-linking of proteins and nucleic acids by its oxidization products. DHI caused a certain level of apoptosis, as indicated by DNA fragmentation and Annexin V staining. After DHI treatment, actin underwent abnormal remodeling which may change cytoskeleton, polarize cell, rupture membrane, and trigger cell death.

3. Regulation of immune response by a serpin from *M. sexta*

A new serpin gene, *M. sexta* serpin-10, was expressed as a recombinant protein. Its transcript level was higher in nerve system, trachea and fat body than in other tissues. The mRNA level did not change much during 4^{th} and 5^{th} instar larvae stages, but decreased remarkably in middle and late pupa stage. In adult stage, its expression was recovered. Expression of *M. sexta* serpin-10 was suppressed in fat body after an immune challenge, suggesting that it was related to antimicrobial response in an unusual way. *M. sexta* serpin-10 level was relatively stable in hemolymph. It formed a covalent complex with an unknown hemolymph protease. *M. sexta* HP1 was found in the immune complex via non-covalent association.

REFERENCES

Abdel-latief M, Hilker M. 2008. Innate immunity: eggs of Manduca sexta are able to respond to parasitism by Trichogramma evanescens. Insect Biochem Mol Biol. 38, 136-145.

Abraham EG, Pinto SB, Ghosh A, Vanlandingham DL, Budd A, Higgs S, Kafatos FC, Jacobs-Lorena M, Michel K. (2005) An immune-responsive serpin, SRPN6, mediates mosquito defense against malaria parasites. Proc Natl Acad Sci U S A. 102:16327-16332.

Aggarwal K, Silverman N. (2008) Positive and negative regulation of the Drosophila immune response. BMB Rep. 41:267-277.

Ahmad-Nejad P, Häcker H, Rutz M, Bauer S, Vabulas RM, Wagner H. 2002 Bacterial CpG-DNA and lipopolysaccharides activateToll-like receptors at distinct compartments Eur J Immunol. 32(7):1958-68.

Akira S, Uematsu S, Takeuchi O. (2006) Pathogen recognition and innate immunity. Cell 124:783-801.

An C, Ishibashi J, Ragan EJ, Jiang H, Kanost MR. (2009) Functions of Manduca Sexta hemolymph proteinases HP6 and HP8 in two innate immune pathways. J Biol Chem. 284:19716-19726.

Ancans J, Tobin DJ, Hoogduijn MJ, Smit NP, Wakamatsu K, Thody AJ. 2001 Melanosomal pH controls rate of melanogenesis, eumelanin/phaeomelanin ratio and melanosome maturation in melanocytes and melanoma cells. Exp Cell Res. 268(1):26-35.

Arkane Y, Muthukrishnan S, Beeman RW, Kanost MR, Kramer KJ. (2005) Laccase 2 is the phenoloxidase gene required for beetle cuticle tanning. Proc Natl Acad Sci U S A 102:11337-11342.

Arzillo M, Pezzella A, Crescenzi O, Napolitano A, Land EJ, Barone V, d'Ischia M. 2010 Cyclic structural motifs in 5,6-dihydroxyindole polymerization uncovered: biomimetic modular buildup of a unique five-membered macrocycle. Org Lett 12(14):3250-3.

Ashid M, Brey PT. (1997) Recent advances on the research of the insect prophenoloxidase cascade. In: Brey, P.T., Hultmark, D. (Eds.), Molecular Mechanisms of Immune Responses in Insects. Chapman &Hall, London, pp. 135-172.

Aso Y, Kramer KJ, Hopkins TL, Whitzel SZ. (1984) Properties of tyrosinase and dopa quinone imine conversion factor from pharate pupal cuticle of Manduca sexta. Insect Biochem. 14:463-472.

Barrett AJ, Rawlings ND. (2001). Evolutionary lines of cysteine peptidases. Biol Chem 382:727-733.

Beck MH, Strand MR. 2007. A novel polydnavirus protein inhibits the insect prophenoloxidase activation pathway. Proc Natl Acad Sci U S A. 104, 19267-19272.

Berkenpas MB, Lawrence DA, Ginsburg D (1995) Molecular evolution of plasminogen activator inhibitor-1 functional stability. EMBO J 14:2969-2977.

Bidla G, Lindgren M, Theopold U, Dushay MS. (2005) Hemolymph coagulation and phenoloxidase in Drosophila larvae. Dev Comp Immunol 29:669-679

Cao C, Lawrence DA, Li Y, Von Arnim CA, Herz J, Su EJ, Makarova A, Hyman BT, Strickland DK, Zhang L. (2006) Endocytic receptor LRP together with tPA and PAI-1 coordinates Mac-1-dependent macrophage migration. EMBO J 25:1860-1670

Carrell RW, Owen M. (1985) Plakalbumin, a1-antitrypsin, antithrombin and the mechanism of inflammatory thrombosis. Nature 317:730-732.

Cerenius L, Söderhäll K. (2004) The prophenoloxidase-activating system in invertebrates. Immunol Rev 198:116–126.

Cerenius, L., Lee, B.L., Söderhäll, K. 2008. The proPO-system: pros and cons for its role in invertebrate immunity. Trends in Immunology 29, 263-271.

Cheng TC, Zhang YL, Liu C, Xu PZ, Gao ZH, Xia QY, Xiang ZH. (2008) Identification and analysis of Toll-related genes in the domesticated silkworm, Bombyx mori. Dev Comp Immunol. 32:464-475.

Christophides GK, Zdobnov E, Barillas-Mury C, Birney E, Blandin S, Blass C, Brey PT, Collins FH, Danielli A, Dimopoulos G, Hetru C, Hoa NT, Hoffmann JA, Kanzok SM, Letunic I, Levashina EA, Loukeris TG, Lycett G, Meister S, Michel K, Moita LF, Müller HM, Osta MA, Paskewitz SM, Reichhart JM, Rzhetsky A, Troxler L, Vernick KD, Vlachou D, Volz J, von Mering C, Xu J, Zheng L, Bork P, Kafatos FC. (2002) Immunity-related genes and gene families in Anopheles gambiae. Science 298:159-165.

Church FC, Cunningham DD, Ginsburg D, Ho man M, Stone SR, Tollefsen DM, editors. Chemistry and biology of serpins. New York: Plenum Press, 1997.

Clark KD, Lu Z, Strand MR. 2010 Regulation of melanization by glutathione in the moth Pseudoplusia includens. Insect Biochem Mol Biol. 40(6):460-7

D'Acquisto F, Carnuccio R, d'Ischia M, Misuraca G. 1995. 5,6-Dihydroxyindole-2-carboxylic acid, a diffusible melanin precursor, is a potent stimulator of lipopolysaccharide-induced production of nitric oxide by J774 macrophages. Life Sci. 57, PL401-6.

De Clercq E. 2002 New anti-HIV agents and targets. Med Res Rev. 22(6):531-65.

De Gregorio E, Han SJ, Lee WJ, Baek MJ, Osaki T, Kawabata S, Lee BL, Iwanaga S, Lemaitre B, Brey PT. (2002) An immune-responsive serpin regulates the melanization cascade in Drosophila. Dev Cell 3, 581-592

De Gregorio E, Spellman PT, Tzou P, Rubin GM, Lemaitre B. (2002) The Toll and Imd pathways are the major regulators of the immune response in Drosophila. EMBO J 21:2568-2579.

Dupas S, Gitau CW, Branca A, Le Rü BP, Silvain JF. Evolution of a polydnavirus gene in relation to parasitoid-host species immune resistance. J Hered. 2008 Sep-Oct;99(5):491-9.

Egelund R, Rodenburg K, Andreasen P, Rasmussen M, Guldberg R, Petersen T. (1998) An ester bond linking a fragment of a serine proteinase to its serpin inhibitor. Biochemistry 37:6375–6379.

Elliott PR, Lomas DA, Carrell RW, Abrahams JP. (1996) Inhibitory conformation of the reactive loop of alpha 1-antitrypsin. Nat Struct Biol 3:676-681.

Ellman GL, Courtney KD, Andres V Jr, Feather-Sone RM. (1961) A new and rapid colorimetric determination of acetylcholinesterase activity. Biochem Pharmacol. 7:88-95.

Gallone A, Sagliano A, Guida G, Ito S, Wakamatsu K, Capozzi V, Perna G, Zanna P, Cicero R. 2007 The melanogenic system of the liver pigmented macrophages of Rana esculenta L.--tyrosinase activity.Histol Histopathol. 22(10):1065-75.

Gan H., Jiang H., Kanost M.R. (2001) A bacteria-induced, intracellular serpin in granular hemocytes of Manduca sexta. Insect Biochem Mol Biol 31:887-898

Gao JR., Kambhampati S., Zhu KY. (2002) Molecular cloning and characterization of a greenbug (Schizaphis graminum) cDNA encoding acetylcholinesterase possibly evolved from a duplicate gene lineage. Insect Biochem Mol Biol 32:765–775.

Gasteiger E, Gattiker A, Hoogland C, Ivanyi I, Appel RD, Bairoch A. (2003) ExPASy: the proteomics server for in-depth protein knowledge and analysis. Nucleic Acids Res 31:3784-3788.

Geer LY, Domrachev M, Lipman DJ, Bryant SH. (2002) CDART: protein homology by domain architecture. Genome Res 12:1619-1623.

Gettins P (2002). Serpin structure, mechanism, and function. Chem Rev 102:4751-804.

Gill SS, Salt AN. 1997 Quantitative differences in endolymphatic calcium and endocochlear potential between pigmented and albino guinea pigs. Hear Res;113:191–197

Gillespie JP, Kanost MR, Trenczek T. (1997) Biological mediators of insect immunity. Ann Rev Entomol 42:611-643.

Gillespie, J.P., Kanost, M.R., Trenczek, T., 1997. Biological mediators of insect immunity. Ann. Rev. Entomol. 42, 611-643.

Gooptu B, Hazes B, Chang WS, Dafforn TR, Carrell RW, Read RJ, Lomas DA. (2000) New inactive conformation of the serpin a1-antichymotrypsin indicates two stage insertion of the reactive loop; Implications for inhibitory function and conformational disease. Proc Natl Acad Sci 97:67–72.

Gorman MJ, Wang Y, Jiang H, Kanost MR. (2007) Manduca sexta hemolymph proteinase 21 activates prophenoloxidase-activating proteinase 3 in an insect innate immune response proteinase cascade. J Biol Chem 282:11742-11749.

Gulii V, Dunphy GB, Mandato CA. (2009) Innate hemocyte responses of Malacosoma disstria larvae (C. Insecta) to antigens are modulated by intracellular cyclic AMP. Dev Comp Immunol 33:890-900.

Gupta S, Wang Y, Jiang H. (2005) Manduca sexta prophenoloxidase (proPO) activation requires proPO-activating proteinase (PAP) and serine proteinase homologs (SPHs) simultaneously. Insect Biochem Mol Biol 35:241-248

Gupta S, Wang Y, Jiang H. (2005) Purification and characterization of Manduca sexta prophenoloxidase-activating proteinase-1, an enzyme involved in insect immune responses. Protein Expr Purif 39:261-268.

Harrop SJ, Jankova L, Coles M, Jardine D, Whittaker JS, Gould AR, Meister A, King GC, Mabbutt BC, Curmi PM. (1999) The crystal structure of plasminogen activator inhibitor2 at 2.0 AÊ resolution: implications for serpin function. Structure 7:43-54.

Heiduschka P, Blitgen-Heinecke P, Tura A, Kokkinou D, Julien S, Hofmeister S, Bartz-Schmidt KU, Schraermeyer U. 2007 Melanin precursor 5,6-dihydroxyindol: protective effects and cytotoxicity on retinal cells in vitro and in vivo. Toxicol Pathol. 35(7):1030-8.

Hill HZ, Hill GJ. 2000 UVA, pheomelanin and the carcinogenesis of melanoma. Pigment Cell Res. 13 Suppl 8:140-4.

Hillyer JF, Schmidt SL, Christensen BM. (2004) The antibacterial innate immune response by the mosquito Aedes aegypti is mediated by hemocytes and independent of Gram type and pathogenicity. Microbes Infect 6:448-459.

Hopkins PC, Carrell RW, Stone SR. (1993) Effects of mutations in the hinge region of serpins. Biochemistry 32:7650–7657.

Howard J, Hyman AA. 2003 Dynamics and mechanics of the microtubule plus end. Nature. 422(6933):753-8.

Hu Q, Noll RJ, Li H, Makarov A, Hardman M, Cooks RG. (2005) The Orbitrap: a new mass spectrometer. J Mass Spectrometry 40:430-443.

Hunt, G., Kyne, S., Ito, S., Wakamatsu, K., Todd, C., and Thody, A. (1995). Eumelanin and phaeomelanin contents of human epidermis and cultured melanocytes. Pigment Cell Res. 8, 202– 208.

Huntington J, Read R, Carrell R. 2000. Structure of a serpin-protease complex shows inhibition by deformation. Nature 407:923-926

Hyman P, Abedon ST. 2010 Bacteriophage host range and bacterial resistance. Adv Appl Microbiol. 2010;70:217-48.

Irving J, Steenbakkers P, Lesk A, Op den Camp H, Pike R, Whisstock J. (2002) Serpins in prokaryotes. Mol Biol Evol 19: 1881-1890.

Irving JA, Pike RN, Dai W, Bromme D, Worrall DM, Silverman GA, Coetzer TH, Dennison C, Bottomley SP, Whisstock JC. (2002) Evidence that serpin architecture intrinsically supports papain- like cysteine protease inhibition: engineering a1-antitrypsin to inhibit cathepsin proteases. Biochemistry 41:4998-5004.

Irving JA, Pike RN, Lesk AM, Whisstock JC. (2000) Phylogeny of the serpin superfamily: implications of patterns of amino acid conservation for structure and function. Genome Res 10:1845-1864.

Iselt M, Holtei W, Hilgard P. 1989. The tetrazolium dye assay for rapid in vitro assessment of cytotoxicity. Arzneimittelforschung J. 39, 747-749.

Ito, S., and Wakamatsu, K. (2008). Review. Chemistry of mixed melanogenesis-Pivotal roles of dopaquinone. Photochem. Photobiol. 84, 582–592.

Jensen JK, Dolmer K, Gettins PG. (1997) Specificity of binding of the low density lipoprotein receptor-related protein (LRP) to different conformational states of the clade E serpins PAI-1 and PN1. Eur J Biochem 248:270-281

Jiang H, Kanost MR. (1997) Characterization and functional analysis of 12 naturally occurring reactive site variants of serpin-1 from Manduca sexta. J Biol Chem. 272:1082-1087.

Jiang H, Wang Y, Huang Y, Mulnix AB, Kadel J, Cole K, Kanost MR. (1996) Organization of serpin gene-1 from Manduca sexta. Evolution of a family of alternate exons encoding the reactive site loop. J Biol Chem 271:28017-28022

Jiang H, Wang Y, Kanost MR. (2001) Proteolytic activation of prophenoloxidase in an insect Manduca sexta. Adv Exp Med Biol 484:313-317.

Jiang H, Wang Y, Yu XQ, Zhu Y, Kanost MR. (2003) Prophenoloxidase-activating proteinase-3 (PAP-3) from Manduca sexta hemolymph: a clip-domain serine proteinase regulated by serpin-1J and serine proteinase homologs. Insect Biochem Mol Biol 33:1049-1060.

Johnson DJ, Li W, Adams TE, Huntington JA. (2006) Antithrombin-S195A factor Xa-heparin structure reveals the allosteric mechanism of antithrombin activation. EMBO J 25:2029-2037.

Kan H, Kim CH, Kwon HM, Park JW, Roh KB, Lee H, Park BJ, Zhang R, Zhang J, Söderhäll K, Ha NC, Lee BL. (2008) Molecular control of phenoloxidase-induced melanin synthesis in an insect. J Biol Chem 283:25316-23.

Kanost MR, Jiang H, Yu XQ. (2004) Innate immune responses of a lepidopteran insect, Manduca sexta. Immunol Rev 198:97–105.

Kanost MR. (1999) Serine proteinase inhibitors in arthropod immunity. Dev Comp Immunol 23:291-301.

Kanost, M.R., Jiang, H., Yu, X-Q., 2004. Innate immune responses of a lepidopteran insect, Manduca sexta. Immunol. Rev. 198, 97–105.

Kawai T, Akira S. 2006 Innate immune recognition of viral infection. Nat Immunol. 7(2):131-7.

Kim CH, Kim SJ, Kan H, Kwon HM, Roh KB, Jiang R, Yang Y, Park JW, Lee HH, Ha NC, Kang HJ, Nonaka M, Söderhäll K, Lee BL. (2008) A three-step proteolytic cascade mediates the activation of the peptidoglycan-induced toll pathway in an insect. J Biol Chem 283:7599-7607.

Kim CH, Park JW, Ha NC, Kang HJ, Lee BL. (2008) Innate immune response in insects recognition of bacterial peptidoglycan and amplification of its recognition signal. BMB Rep. 41:93-101.

Kim YS, Ryu JH, Han SJ, Choi KH, Nam KB, Jang IH, Lemaitre B, Brey PT, Lee WJ. (2000) Gram-negative bacteria-binding protein, a pattern recognition receptor for lipopolysaccharide and beta-1,3-glucan that mediates the signaling for the induction of innate immune genes in Drosophila melanogaster cells. J Biol Chem 275:32721-32727.

Kohler LJ, Carton Y, Mastore M, Nappi AJ. 2007. Parasite suppression of the oxidations of eumelanin precursors in Drosophila melanogaster. Arch. Insect Biochem. Physiol. 66, 64-75.

Kuntumalla S, Braisted JC, Huang ST, Parmar PP, Clark DJ, Alami H, Zhang Q, Donohue-Rolfe A, Tzipori S, Fleischmann RD, Peterson SN, Pieper R. (2009) Comparison of two label-free global quantitation methods, APEX and 2D gel electrophoresis, applied to the Shigella dysenteriae proteome. Proteome Sci 7:22.

Kuzina LV, Peloquin JJ, Vacek DC, Miller TA. (2001) Isolation and identification of bacteria associated with adult laboratory Mexican fruit flies, Anastrepha ludens (Diptera: Tephritidae). Curr Microbiol 42:290-294.

Land, E.J., and Riley, P.A. (2000). Spontaneous redox reactions of dopaquinone and the balance between the eumelanic and phaeomelanic pathways. Pigment Cell Res. 13, 273–277.

Lata S, Raghava GP. (2008) PRRDB a comprehensive database of pattern-recognition receptors and their ligands. BMC Genomics 9:180.

Lavine MD, Strand MR. (2002) Insect hemocytes and their role in immunity. Insect Biochem Mol Biol 32:1295-1309.

Leclerc V, Pelte N, El Chamy L, Martinelli C, Ligoxygakis P, Hoffmann JA, Reichhart JM. (2006) Prophenoloxidase activation is not required for survival to microbial infections in Drosophila. EMBO Rep 7:231-235.

Leclerc V, Pelte N, El Chamy L, Martinelli C, Ligoxygakis P, Hoffmann JA, Reichhart JM. 2006. Prophenoloxidase activation is not required for survival to microbial infections in Drosophila. EMBO Rep. 7, 231-235.

Lemaitre B, Hoffmann J. (2007) The host defense of Drosophila melanogaster. Annu Rev Immunol 25:697-743.

Lemaitre B, Nicolas E, Michaut L, Reichhart JM, Hoffmann JA. (1996) The dorsoventral regulatory gene cassette spätzle/Toll/cactus controls the potent antifungal response in Drosophila adults. Cell 86:973-983.

Letunic I, Doerks T, Bork P. (2009) SMART 6: recent updates and new developments. Nucleic Acids Res 37:D229-232.

Li H, Tang H, Sivakumar S, Philip J, Harrison RL, Gatehouse JA, Bonning BC. 2008. Insecticidal activity of a basement membrane-degrading protease against Heliothis virescens (Fabricius) and Acyrthosiphon pisum (Harris). J Insect Physiol. 54, 777-789.

Li J, Wang Z, Canagarajah B, Jiang H, Kanost M, Goldsmith EJ. (1999) The structure of active serpin 1K from Manduca sexta. Structure 7:103-109.

Li W, Johnson DJ, Esmon CT, Huntington JA. (2004) Structure of the antithrombin-thrombin-heparin ternary complex reveals the antithrombotic mechanism of heparin. Nat Struct Mol Biol 11:857-862.

Li ZZ, Li CR, Huang B, Fan MZ. (2001) Discovery and demonstration of the teleomorph of Beauveria bassiana (Bals.) Vuill., an important entomogenous fungus. Chinese Science Bulletin 46:751-753

Lindahl T, Sigurdardottir O, Wiman B. (1989) Stability of plasminogen activator inhibitor-1 (PAI-1). Thromb Haemost 62: 748-751.

Lovallo N, Cox-Foster DL. 1999 Alteration in FAD-glucose dehydrogenase activity and hemocyte behavior contribute to initial disruption of Manduca sexta immune response to Cotesia congregata parasitoids. J Insect Physiol. 45(12):1037-1048.

Lu Z, Beck MH, Wang Y, Jiang H, Strand MR. 2008. The viral protein Egf1.0 is a dual activity inhibitor of prophenoloxidase-activating proteinases 1 and 3 from Manduca sexta. J Biol Chem. 283, 21325-21333.

Lu Z, Jiang H. (2008) Expression of Manduca sexta serine proteinase homolog precursors in insect cells and their proteolytic activation. Insect Biochem Mol Biol 38:89-98.

Lu Z, Jiang H.2007 Regulation of phenoloxidase activity by high- and low-molecular-weight inhibitors from the larval hemolymph of Manduca sexta. Insect Biochem Mol Biol. 37(5):478-85.

M. Miranda, F. Amicarelli, A. Bonfigli, A. Poma, O. Zarivi and A. Arcadi 1990. Mutagenicity test for unstable compounds, such as 5, 6-dihydroxyindole, using an Escherichia coli HB101/pBR322 transfection system, Mutagenesis 5, 251-256.

McNeil J, Cox-Foster D, Slavicek J, Hoover K. 2010 Contributions of immune responses to developmental resistance in Lymantria dispar challenged with baculovirus. J Insect Physiol. 56(9):1167-77.

Michel K, Suwanchaichinda C, Morlais I, Lambrechts L, Cohuet A, Awono-Ambene PH, Simard F, Fontenille D, Kanost MR, Kafatos FC. 2006. Increased melanizing activity in Anopheles gambiae does not affect development of Plasmodium falciparum. Proc Natl Acad Sci U S A. 103, 16858-63.

Mottonen J, Strand A, Symersky J, Sweet RM, Danley DE, Geoghegan KF, Gerard RD, Goldsmith EJ. (1992) Structural basis of latency in plasminogen activator inhibitor-1. Nature 355:270-273.

Napolitano, A., Di Donato, P., Prota, G., and Land, E.J. (1999). Transient quinonimines and 1,4-benzothiazines of pheomelanogenesis: new pulse radiolytic and spectrophotometric evidence. Free Radic. Biol. Med. 27, 521–528.

Nappi AJ, Christensen BM. (2005) Melanogenesis and associated cytotoxic reactions: applications to insect innate immunity. Insect Biochem Mol Biol 35:443-459.

Nappi AJ, Vass E, Carton Y, Frey F. 1992. Identification of 3,4-dihydroxyphenylalanine, 5,6-dihydroxyindole, and N-acetylarterenone during eumelanin formation in immune reactive larvae of Drosophila melanogaster. Arch Insect Biochem Physiol. 20, 181-91.

Nappi, A.J., Christensen, B.M., 2005. Melanogenesis and associated cytotoxic reactions: applications to insect innate immunity. Insect Biochem. Mol. Biol. 35, 443-459.

Novellino L, Napolitano A, Prota G. 1999. 5,6-Dihydroxyindoles in the fenton reaction: a model study of the role of melanin precursors in oxidative stress and hyperpigmentary processes. Chem Res Toxicol. 12, 985-92.

Page RD. (2002) Phylogenetic trees using TreeView. Curr Protoc Bioinformatics Chapter 6:Unit 6.2.

Pennacchio, F. and M.R. Strand. 2006. Evolution of developmental strategies in parasitic Hymenoptera. Annu. Rev. Entomol. 51, 233-258.

Pinto SB, Kafatos FC, Michel K. (2008) The parasite invasion marker SRPN6 reduces sporozoite numbers in salivary glands of Anopheles gambiae. Cell Microbiol 10:891-898.

Ponting CP, Schultz J, Milpetz F, Bork P. (1999) SMART: identification and annotation of domains from signalling and extracellular protein sequences. Nucleic Acids Res. 27:229-232.

Popham HJ, Shelby KS, Brandt SL, Coudron TA. 2004 Potent virucidal activity in larval Heliothis virescens plasma against Helicoverpa zea single capsid nucleopolyhedrovirus. J Gen Virol. 85(Pt 8):2255-61.

Potempa J, Korzus E, Travis J. The serpin superfamily of proteinase inhibitors: structure, function, and regu-lation. J Biol Chem 269:15957-15960.

Rawlings ND, Tolle DP, Barrett AJ. (2004) Evolutionary families of peptidase inhibitors. Biochem J 378:705-716.

Riedl SJ, Salvesen GS. 2007 The apoptosome: signalling platform of cell death. Nat Rev Mol Cell Biol. 8(5):405-13.

Riesz JJ, Gilmore JB, McKenzie RH, Powell BJ, Pederson MR, Meredith P. 2007 Phys Rev E Stat Nonlin Soft Matter Phys. 76(2 Pt 1):021915.

Royet J, Dziarski R. (2007) Peptidoglycan recognition proteins pleiotropic sensors and effectors of antimicrobial defences. Nat Rev Microbiol 5:264-277.

Saejeng A, Tidbury H, Siva-Jothy MT, Boots M. 2010 Examining the relationship between hemolymph phenoloxidase and resistance to a DNA virus, Plodia interpunctella granulosis virus (PiGV). J Insect Physiol. 56(9):1232-6.

Schecter, I, Berger, A. (1967) On the size of the active site in proteases. I. Papain. Biochem. Biophys. Res. Commun. 27:157-162.

Scherfer C, Tang H, Kambris Z, Lhocine N, Hashimoto C, Lemaitre B. (2008) Drosophila Serpin-28D regulates hemolymph phenoloxidase activity and adult pigmentation. Dev Biol 323:189-196.

Schultz J, Milpetz F, Bork P, Ponting CP. (1998) SMART, a simple modular architecture research tool: identification of signaling domains. Proc Natl Acad Sci U S A 95:5857-5864.

Shelby KS, Popham HR. 2006. Plasma phenoloxidase of the larval tobacco budworm, Heliothis virescens, is virucidal. J. Insect Sci. 6:13

Silverman GA, Bird PI, Carrell RW, Church FC, Coughlin PB, Gettins PG, Irving JA, Lomas DA, Luke CJ, Moyer RW, Pemberton PA, Remold-O'Donnell E, Salvesen GS, Travis J, Whisstock JC. (2001) The serpins are an expanding superfamily of structurally similar but functionally diverse proteins. J Biol Chem 276:33293-33296.

Simon JD, Peles D, Wakamatsu K, Ito S. 2009 Current challenges in understanding melanogenesis: bridging chemistry, biological control, morphology, and function. Pigment Cell Melanoma Res. 22(5):563-79.

Söderhäll K, Cerenius L. (1998) Role of the prophenoloxidase-activating system in invertebrate immunity. Curr Opin Immunol. 10(1):23-8.

Soukup SF, Culi J, Gubb D. (2009) Uptake of the necrotic serpin in Drosophila melanogaster via the lipophorin receptor-1. PLoS Genet 5:e1000532.

Stein PE, Carrell RW. (1995) What do dysfunctional serpins tell us about molecular mobility and disease? Nat Struct Biol 2:96-113.

Sugumaran M. (2002) Comparative biochemistry of eumelanogenesis and the protective roles of phenoloxidase and melanin in insects. Pigment Cell Res 15, 2-9.

Tanaka H, Ishibashi J, Fujita K, Nakajima Y, Sagisaka A, Tomimoto K, Suzuki N, Yoshiyama M, Kaneko Y, Iwasaki T, Sunagawa T, Yamaji K, Asaoka A, Mita K,

Yamakawa M. (2008) A genome-wide analysis of genes and gene families involved in inn ate immunity of Bombyx mori. Insect Biochem Mol Biol 38:1087-1110.

Tang H, Kambris Z, Lemaitre B, Hashimoto C. Two proteases defining a melanization cascade in the immune system of Drosophila. J Biol Chem. 2006 Sep 22;281(38):28097-104.

Thody, A. J., Higgins, E. M., Wakamatsu, K., Ito, S., Burchill, S. A., and Marks, J. M. (1991). Pheomelanin as well as eumelanin is present in human epidermis. J. Invest. Dermatol. 97, 340–344.

Thompson JD, Gibson TJ, Plewniak F, Jeanmougin F, Higgins DG. (1997) The ClustalX windows interface: flexible strategies for multiple sequence alignment aided by quality analysis tools. Nucleic Acids Res 24:4876-4882

Thompson JD, Higgins DG, Gibson TJ. (1994) CLUSTAL W: improving the sensitivity of progressive multiple sequence alignment through sequence weighting, positions-specific gap penalties and weight matrix choice. Nucleic Acids Res 22:4673-4680.

Tong Y, Jiang H, Kanost MR. (2005) Identification of plasma proteases inhibited by Manduca sexta serpin-4 and serpin-5 and their association with components of the prophenol oxidase activation pathway. J Biol Chem 280:14932-14942.

Tong Y, Kanost MR. (2005) Manduca sexta serpin-4 and serpin-5 inhibit the prophenol oxidase activation pathway: cDNA cloning, protein expression, and characterization. J Biol Chem 280:14923-14931.

Trudeau D, Washburn J.O., Volkman, L.E., 2001. Central role of hemocytes in Autographa californica M nucleopolyhedrovirus pathogenesis in Heliothis virescens and Helicoverpa zea. J. Virol. 75, 996–1003.

Tsukada H, Blow DM. (1985) Structure of alpha-chymotrypsin refined at 1.68 A resolution. J Mol Biol 184: 703-711.

Wang Y, Jiang H. (2004a) Prophenoloxidase (proPO) activation in Manduca sexta: an analysis of molecular interactions among proPO, proPO-activating proteinase-3, and a cofactor. Insect Biochem Mol Biol 34:731-742.

Wang Y, Jiang H. (2004b) Purification and characterization of Manduca sexta serpin-6: a serine proteinase inhibitor that selectively inhibits prophenoloxidase-activating proteinase-3. Insect Biochem Mol Biol 34:387-95.

Wang Y, Jiang H. (2006) Interaction of beta-1,3-Glucan with its recognition protein activates hemolymph proteinase 14, an initiation enzyme of the prophenoloxidase activation system in Manduca sexta. J Biol Chem 281:9271-9278.

Wang Y, Jiang H. (2007) Reconstitution of a branch of the Manduca sexta prophenoloxidase activation cascade in vitro: snake-like hemolymph proteinase 21 (HP21) cleaved by HP14 activates prophenoloxidase-activating proteinase-2 precursor. Insect Biochem Mol Biol 37:1015-1025.

Whisstock J, Bottomley S. (2006) Molecular gymnastics: serpin structure, folding and misfolding. Curr Opin Struct Biol 16:761-768.

Whisstock JC, Pike RN, Jin L, Skinner R, Pei XY, Carrell RW, Lesk AM. (2000b) Conformational changes in serpins. II. The mechanism of activation of antithrombin by heparin. J Mol Biol 301:1287-1305.

Whisstock JC, Skinner R, Carrell RW, Lesk AM. (2000a) Conformational changes in serpins: I. The native and cleaved conformations of alpha(1)-antitrypsin. J Mol Biol 296:685-699.

Wilson R, Chen C, Ratcliffe NA. (1999) Innate immunity in insects: the role of multiple, endogenous serum lectins in the recognition of foreign invaders in the cockroach, Blaberus discoidalis. J Immunol 162:1590-1596.

Wood JM, Jimbow K, Boissy RE, Slominski A, Plonka PM, Slawinski J, Wortsman J, Tosk J. 1999 What's the use of generating melanin? Exp Dermatol;8:153–164

Wysocki VH, Resing KA, Zhang Q, Cheng G. (2005) Mass spectrometry of peptides and proteins. Methods 35:211–222.

Ye S, Cech AL, Belmares R, Bergstrom RC, Tong Y, Corey DR, Kanost MR, Goldsmith EJ. (2001) The structure of a Michaelis serpin-protease complex. Nat. Struct Biol 8:979-983.

Yin L, Zhang C, Qin J, Wang C. 2003 Polydnavirus of Campoletis chlorideae: characterization and temporal effect on host Helicoverpa armigera cellular immune response. Arch Insect Biochem Physiol. 52(2):104-13.

Yu XQ, Jiang H, Wang Y, Kanost MR. (2003) Nonproteolytic serine proteinase homologs are involved in prophenoloxidase activation in the tobacco hornworm, Manduca sexta. Insect Biochem Mol Biol 33:197-208.

Zhang G, Lu ZQ, Jiang H, Asgari S. 2004. Negative regulation of prophenoloxidase (proPO) activation by a clip-domain serine proteinase homolog (SPH) from endoparasitoid venom. Insect Biochem Mol Biol. 34, 477-483.

Zhang Q, Buckle AM, Law RH, Pearce MC, Cabrita LD, Lloyd GJ, Irving JA, Smith AI, Ruzyla K, Rossjohn J, Bottomley SP, Whisstock JC. (2007) The N-terminus of the serpin, tengpin, functions to trap the metastable native state. EMBO Rep 8: 658.

Zhang Q, Law RH, Bottomley SP, Whisstock JC, Buckle AM. (2008) A structural basis for loop C-sheet polymerization in serpins. J Mol Biol 376:1348-59.

Zhao P, Zhu KY, Jiang H. (2010) Heterologous expression, purification, and biochemical characterization of a greenbug (Schizaphis graminum) acetylcholinesterase encoded by a paralogous gene (ace-1). J Biochem Mol Toxicol 24(1):51-9.

Zhao, P., Jiajing Li, Yang Wang, Jiang, H., 2007. Broad-spectrum antimicrobial activity of the reactive compounds generated in vitro by Manduca sexta phenoloxidase. Insect Biochem. Mol. Biol. 37, 952-959.

Zhu Y, Wang Y, Gorman MJ, Jiang H, Kanost MR. (2003) Manduca sexta serpin-3 regulates prophenoloxidase activation in response to infection by inhibiting prophenoloxidase-activating proteinases. J Biol Chem 278:46556-46564

Zou Z, Evans JD, Lu Z, Zhao P, Williams M, Sumathipala N, Hetru C, Hultmark D, Jiang H. (2007) Comparative genomic analysis of the Tribolium immune system. Genome Biol 8:R177.

Zou Z, Jiang H. (2005) Manduca sexta serpin-6 regulates immune serine proteinases PAP-3 and HP8. cDNA cloning, protein expression, inhibition kinetics, and function elucidation. J Biol Chem 280:14341-14348.

Zou Z, Najar F, Wang Y, Roe B, Jiang H. (2008) Pyrosequence analysis of expressed sequence tags for Manduca sexta hemolymph proteins involved in immune responses. Insect Biochem Mol Biol 38:677-682.

Zou Z, Picheng Z, Weng H, Mita K, Jiang H. (2009) A comparative analysis of serpin genes in the silkworm genome. Genomics 93:367-375.

Zou Z, Shin SW, Alvarez KS, Bian G, Kokoza V, Raikhel AS. 2008. Mosquito RUNX4 in the immune regulation of PPO gene expression and its effect on avian malaria parasite infection. Proc Natl Acad Sci U S A. 105, 18454-18459.

APPENDICES

Abbreviations

AMP	antimicrobial peptide
AS	Ammonium sulfate
AS	Ammonium sulfate
BSA	Bovine serum albumin
DAP	meso-diaminopimelic acid
DAPI	4',6-diamidino-2-phenylindole
DHI	5,6-dihydrooxindole
DS	dextran sulfate
F-actin	filamentous actin
GNBP	Gram nagtive binding protein
HP	Hemolymph protease
HT	hydroxyapatite
LB	Luria-Bertani
LpR	lipophorin receptor
LPS	lipopolysaccharide
Ms	manduca sexta
MTT	3-(4,5-dimethylthiazol-2-yl)-2,5-diphenyltetrazolium bromide
NADA	N-acetyldopamine
NBAD	N-β-alanyldopamine
PAE	PPO activation protease
PAGE	polyacrylamide gel electrophoresis
PAI	plasminogen activator inhibitor
PAMP	pathogen-associated molecular patterns
PB	phosphate buffer
PBS	phosphate buffer saline
PGN	peptidoglycan
PGRP	peptidoglycan recognition protein
PI	propidium iodide
PO	phenoloxidase
PPO	prophenoloxidase
PTU	1-phenyl-2-thiourea
RCL	flexible reactive center loop

serpin	serine protease inhibitor
*Sg*AChE1	*Schizaphis graminum* acetylcholinesterase-1
SPC	serpin-protease complexes
SPE	Spätzle-processing enzyme
SPH	serine protease homolog
Spn	serpin
Tm	Tenebrio molitor
β-GRP	β-1,3-glucan recognition protein

Picheng Zhao

Candidate for the Degree of

Doctor of Philosophy

Dissertation: ANTIMICROBIAL ACTIVITIES OF PHENOLOXIDASE-GENERATED REACTIVE COMPOUNDS AND REGULATION OF IMMUNE RESPONSE BY A SERPIN FROM *MANDUCA SEXTA*

Major Field: Entomology

Biographical:

Education:

Received Bachelor in Biochemical Engineering from East China University of Science and Technology, China in June 2001. Completed the requirements for the Doctor of Philosophy in Chemical Engineering at Oklahoma State University, Stillwater, Oklahoma in December, 2010

Experience:

From 2001-2005 Cygen Biotech Co. Ltd., Shanghai, China

Title: Director of Department of Cell and Immunology/ Engineer

Professional Memberships:
ESA

Name: Picheng Zhao Date of Degree: December, 2010

Institution: Oklahoma State University Location: Stillwater, Oklahoma

Title of Study: ANTIMICROBIAL ACTIVITIES OF PHENOLOXIDASE-GENERATED REACTIVE COMPOUNDS AND REGULATION OF IMMUNE RESPONSE BY A SERPIN FROM *MANDUCA SEXTA*

Pages in Study: 95 Candidate for the Degree of Doctor of Philosophy

Major Field: Entomology

Scope and Method of Study: Phenoloxidase (PO) and its activation system are implicated in several defense responses of insects. Upon wounding or infection, inactive prophenoloxidase (proPO) is converted to active PO through a network of serine proteases and their homologs. PO generates reactive compounds such as 5,6-dihydroxyindole (DHI), which have a broad-spectrum antimicrobial activity. The regulation of proteolytic activation cascade of immune response involves serine protease inhibitor (serpin) family molecules. Many serpins are found to play key roles in negatively regulating immune defense system through irreversibly inhibiting target serine proteases, not only to humoral but also to the cellular responses. A new gene, serpin-10, was found in *Manduca sexta* and expressed in insect cell via infection of recombinant baculovirus contain serpin-10 cDNA fragment. The serpin10 antiserum was prepared and used for determining protein level in hemolymph and affinity chromatography to analysis immune complex formation with serpin-10.

Findings and Conclusions: Here we demonstrate that DHI and its spontaneous oxidation products are active against bacteria, fungi, viruses, and parasitic wasp eggs. These results established that proPO activation is an integral component of the insect defense system. A possible mechanism of DHI toxicity is the cross-linking of proteins and nucleic acid via its oxidization products. The transcript level of *M. sexta* serpin-10 is higher in nerve system, trachea, and fat body than in other tissues. The transcriptional level does not change a lot during 4^{th} and 5^{th} instar larval stages, but decreases remarkably in middle and late pupa stage, and then recovers in adults. This gene is suppressed in fat body, which indicates it may have a relationship with immune response to pathogen invasion. The protein level of serpin-10 is quite stable in hemolymph. *M. sexta* serpin10 forms a covalent complex with an unknown serine protease. HP1 is present in the immune complex via non-covalent association.

ADVISER'S APPROVAL: HAOBO JIANG